WESTERN PACIFIC EARTH SCIENCES
Vol.1, No.3, P.297-338, 10 Figs., 8 Tabs., August, 2001

A PRELIMINARY STUDY ON THE RELATIONSHIP BETWEEN ENGINEERING PROPERTIES AND UNIAXIAL COMPRESSIVE STRENGTH OF WEAK SANDSTONES

HONGEY CHEN AND ZER-YE HU

Department of Geosciences, National Taiwan University,Taipei, Taiwan

ABSTRACT

This study applied multiple regression analysis to examine the relationship between engineering characteristics and uniaxial compressive strength of weak sandstones. The results show that as quartz content increases, wave velocity, uniaxial compressive strength and slake durability decrease. When water content increases wave velocity and uniaxial compressive strength of weak sandstones decrease. The laboratory tests revealed that mineral composition mainly includes 50% quartz, 30% matrix and 10% detritus. These results also demonstrate that wave velocity, uniaxial compressive strength and slaking durability of weak sandstones increase with increasing porosity.

Key words: compressive strength, weak sandstone, matrix, detritus

INTRODUCTION

The range of uniaxial compressive strength for weak sandstones is usually between 0. 5Mpa and 25Mpa (GSL, 1970; ISRM, 1981). There are 5 relevant properties in weak rocks: (1) poor cementation between particles, (2) weathering process, (3) tectonics disturbance, and (4) larger empty voids between particles, and (5) mineral composition (Olivera, 1993). Gunsallus and Kulhaway (1984) and Shakoor and Bonelli (1991) found that uniaxial compressive strength has a strongly positive correlation with quartz content. However, Bell (1978), Ulusay *et al.* (1994) thought that quartz content is unrelated to compressive strength. The particles in a sandstone rock are considered to have good cementation if the matrix minerals are quartz or calcite. This strength would be greater than clay matrix (Vutukuri *et al.*, 1974; Barton *et al.*, 1993).

Uniaxial compressive strength of the weak sandstones decreases when particle size, porosity and water content increase (Bell and Culshaw, 1993; Yuan, 1996). Hugman and Freidman (1979), Ondera and Asoka (1980) Dobereiner and de Freitas (1986) and Bell and Culshaw (1993) also found that rock strength decreases when particle size increases. Strength of weak sandstones increases as density increases.

This paper presents preliminary results of various experimental tests of weak sandstones and quantifies the relationships between physical factors and their uniaxial compressive strengths using multiple regression analyses. These factors include physical properties and mineral compositions. The weak sandstones were part of the Kweichulin Formation and the Shihti Formation in the eastern end of the Taipei Basin. The study area is located near the intersection of the hilly and plain areas of the eastern part of Taipei City.

GEOLOGICAL CONDITIONS

The Shihti Formation and the south side of the Kweichulin Formation of the Miocene age (Fig. 1), are two identifiable layers distributed on both sides of the Taipei fault in the study area (Huang, 1988). The strike of the Kweichulin Formation ranges from N45^{0}E to N50^{0}E, and the dip is southward at 30^o. The strike of the Shihti Formation ranges from N65^{0}W to N75^{0}E, and the dip is southward at 80^0. The outcrop of the basement appears in a fractured condition. The Shihti Formation is the most important formation for coal in the northwestern part of Taiwan. Its age is around 18.8 to 20 Ma.

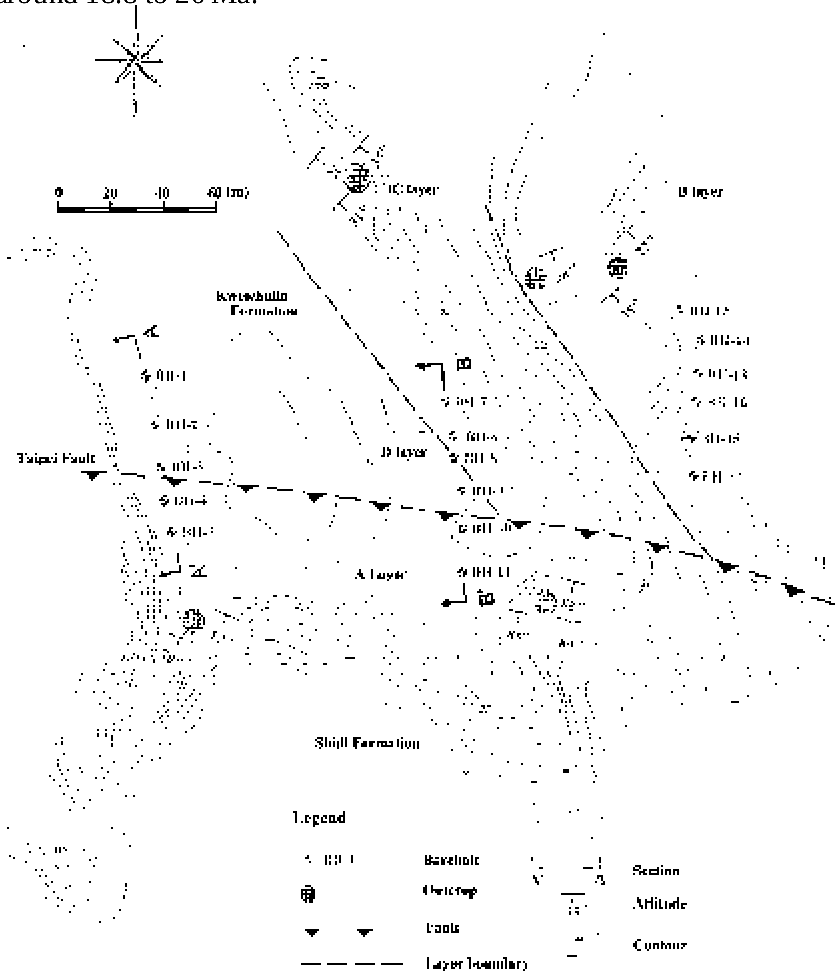

Figure 1.Geological map of the study area showing borehole locations.

The most common feature of both formations is the presence of laminated, interbedded, gray-black shale and white sandstone. The thickness of lamination is only a few millimeters to a few centimeters. The sedimentary environment of this formation resulted from a shore tide plain, a delta or a swamp-like area. Shale in the Shihti Formation is dark gray to gray-black and rich in carbon content. Sandstone is rich in feldspar and consists of small to medium sized particles. It usually appears light gray to white.

The Kweichulin Formation, in northern Taiwan, ranges from 4.0 to 8.0 Ma and is of the Mid-Miocene age (Ho, 1986). It is mostly fine-grained and characterized by abundance of clayey, massive sandstones. Light gray sandstone is interbedded with dark gray shale.

This study took core samples of 54.7 mm diameter from 17 boreholes. Cores from boreholes BH-5, BH-11, BH-4 and BH-10, clearly show lamination and coal layers—common characteristics of the Shihti Formation.

Boreholes BH-1, BH-2, BH-3, BH-6, BH-7, BH-8, BH-9, BH-12, BH-13, BH-14, BH-15, BH-16 and BH-17 mainly provide gray silty massive sandstones of the Kweichulin Formation. It is characterized by loose cementation and contains interbedded sandstone and shale. Two sections of A-A' and B-B' show the thickness of rock formations in the study area (Figures 2 (a) and (b)). Lithological characteristics of various rock layers of the study area are described in Table 1.

Table 1. Stratigraphic description of the study area.

Formation	Layer	Description
Shihti Formation	A	The rock type consists of white to gray sandstone and shale with interbedded coal. It is more than 30 meters thick. This layer is distributed on the south part of the Taipei fault and formed in a fractured condition.
Kweichulin Formation	B	This layer is more than 40 meters thick. This layer is distributed on the northern part of the Taipei fault. The rock cementation is poor and the rock mass is fractured. The rock is fine to medium grained, and lightly greenish-gray to dark gray massive sandstone interbedded with gray dark shale. The massive sandstone has a high clay content.
	C	The thickness of this layer ranges from 15 meters to 25 meters. This layer is distributed on the north part of the Taipei fault and is below the layer B. The rock type is fine to medium grained, massive sandstone interbedded with dark gray shale.
	D	The thickness of this layer is more than 40 meters. It is distributed on the northern part of the Taipei fault and is underneath layer C. The rock type is fine to medium grained, massive and muddy sandstone interbedded with dark gray shale. This layer contains some shell fossils. The rock cementation is poor and has highly fractured.

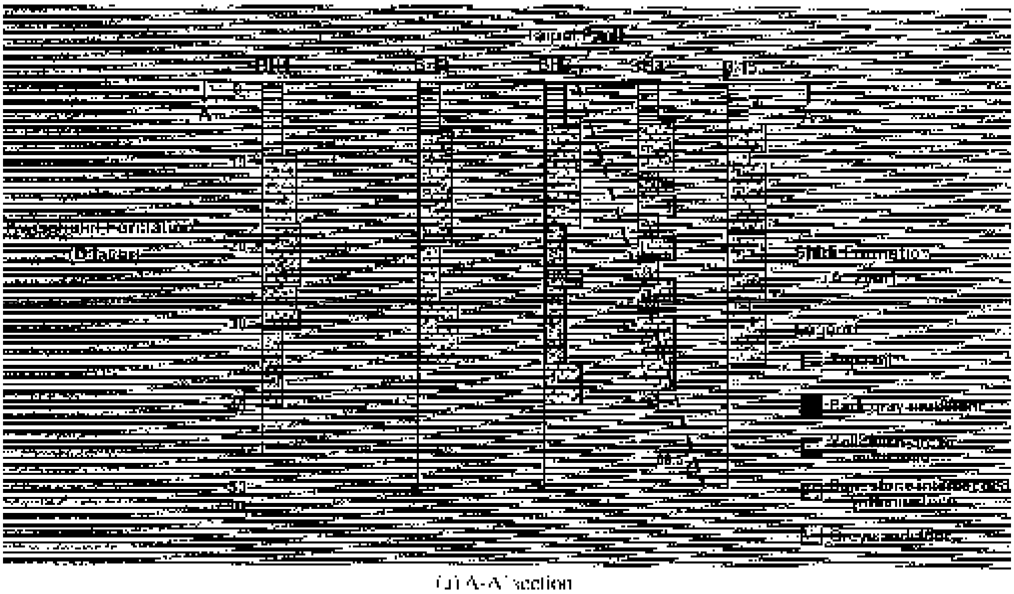

Figure 2a. Columnar sections showing the Kweichulin Formation and the Shihti Formation, based on boreholes data, in relation to the Taipei Fault.

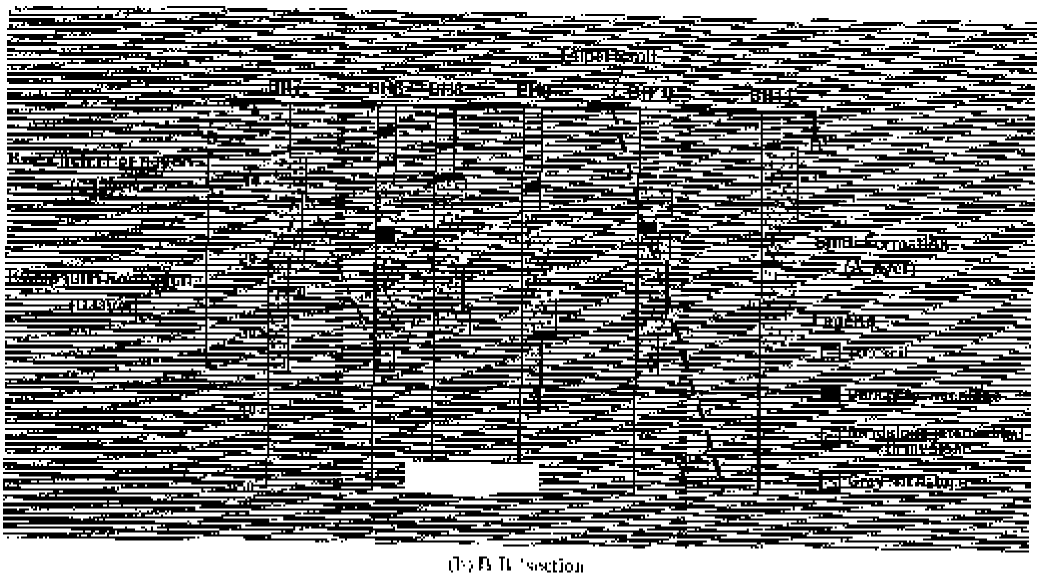

Figure 2b. Columnar sections showing the Kweichulin Formation and the Shihti Formation, based on boreholes data, in relation to the Taipei Fault. (Cont'd).

The boreholes penetrated into four layers of differing geomaterial strata in the Shihti and Kweichulin Formations of the study area. The 30 meters thick Layer A of the Shihti Formation is distributed on the south side of the Taipei Fault. The rock types are white to gray clayey massive sandstone, coal, and interbedded with dark gray shale.

Layers B, C, and D are distributed on the north side of the Taipei Fault. They belong to the Kweichulin Formation. Layers B and D are more than 40 meters thick. They are composed of fine to medium grained, light greenish-gray to dark gray, clayey, massive sandstone interbedded with gray shale. Layer C is 15 to 25 meters thick. Rock types consist of fine to medium grained, gray, clayey massive sandstone. All of the rock cores appear poorly cemented and somewhat fractured.

EXPERIMENTAL METHODS

The study used various experimental methods to explore the engineering characteristics of the sandstone samples, which are 54mm in diameter from all the boreholes. Tests include determination of physical properties, wave velocity, uniaxial compressive strength, and slake durability.

Physical properties of water content, porosity and density were determined according to the procedures recommended in ISRM (1981). Wave velocity was obtained by application of ultrasonic compressive wave pulses to the testing samples in accordance with the procedures described in ASTM (1980).

A compressive wave generator was attached to the testing sample. Wave velocity was measured as travel time through the core sample from the generator to a receiver at the opposite end. Longitudinal wave and shear wave velocities were obtained from the applicable calculation according to the above standard procedures.

Uniaxial compressive strength testing was determined using a uniaxial compression test machine in accordance with the specifications in ISRM (1981). Slake durability tests included two cycles of testing for each sample, following the specifications in ISRM (1981).

RESULTS

Mineral composition

Mineral composition of the weak sandstones consists of quartz, detritus and matrix materials as revealed in an examination of 59 thin sections. Feldspar content was found to be less than 10.7%. Calcite and other minerals have a minor distribution in the rock samples.

Quartz content varies in the Shihti Formation, ranging from 21.1% to 62.7%. Detritus content varies from 3.7% to 17.3%, and matrix content from 19.8% to 71.9%. These results show a large variability in mineral composition (Tab. 2).

Mineral composition of the Kweichulin Formation also varies widely. Quartz ranges from 25.0% to 72.3%, detritus from 4.3% to 26.7%, matrix from 4.7% to 64.3%. The average amount of detritus is higher in the Kweichilun Formation than in the Shihti Formation. Feldspar content is higher in the Shihti Formation. In general, the samples have approximately 30% matrix content, primarily of clay material.

Table 2. Mineral composition of the various layers of weak sandstones of the study area.

	Quartz (%)	Feldspar (%)	Calcite (%)	Detritus (%)	Matrix (%)	Others (%)
Shihti Formation (A layer)	21.1～62.7	1.5～10.3	0～2.7	3.7～17.3	19.8～71.9	0～4.7
Kweichulin Formation (B layer)	34.3～69.7	1.3～7.3	0～2.3	4.3～19.2	13.7～51.3	0～4.3
Kweichulin Formation (C layer)	37.7～56.5	0.3～3.0	0～25.2	13.7～26.7	1.7～34.3	0～1
Kweichulin Formation (D layer)	25.0～72.3	2.0～10.7	0～12.7	7.0～19.3	4.7～64.3	0～2.3

The results of X-ray diffraction demonstrate that the Shihti Formation has a higher content of kaolinite (not including chorite). Both kaolinite and chorite are distributed in very similar proportions in the Kweichulin Formation. No smecite was found in the Shihti Formation but it is present in the Kweichulin Formation.

Illite content in the Shihti Formation is less than that in the Kweichulin Formation. Smecite and kaolinite proportions in layer D of the Kweichulin Formation are less than those in layers B and C. However, chlorite content is higher in this formation (Tab. 3).

Physical properties

The results of physical property analyses (including water content, porosity and density) are shown in Table 4.

The average water content of the weak sandstones across all samples in the study area is under 3.5%. In general, layer A in the Shihti Formation has higher water content, and layer C in the Kweichulin Formation has lower water content. The average porosity of the weak sandstones ranges from 3.2% to 26.5%. There is little difference in the porosity of the individual layers.

The average density of the weak sandstones ranges from 1.95g/cm^3 and 2.60g/cm^3. Layers C and D of the Kweichulin Formation average 2.40g/cm^3 and 2.23g/cm^3, respectively. Layer C of the Kweichulin Formation has a higher density. These results match the porosity values and the thin section measurements.

Table 3. Results of semi-quantitative analysis of clay minerals in various layers.

	Smectite (%)	Illite (%)	Chlorite (%)	Kaolinite (%)
Shihti Formation (A layer)	0	15.8～53.8	0～1.1	46.2～84.2
Kweichulin Formation (B layer)	8.1～22.3	42.4～54.1	11.1～26.3	18.5～30.3
Kweichulin Formation (C layer)	5.1～17.4	40.3～52.1	20.6～20.7	21.7～22.1
Kweichulin Formation (D layer)	0～20.1	18.36～54.5	19.6～53.3	0～26.4

Table 4. The physical properties of various layers of the study area.

	Water content (%)	Porosity (%)	Density (g/cm³)	Specific gravity
Shihti Formation (A layer)	0.61～3.43	4～19.5	2.14～2.39	2.54～2.68
Kweichulin Formation (B layer)	0.43～2.37	7.5～26.5	1.95～2.45	2.55～2.65
Kweichulin Formation (C layer)	0.17～1.05	3.2～13.4	2.33～2.60	2.61～2.68
Kweichulin Formation (D layer)	0.45～3.5	8.0～25.1	2.00～2.43	2.58～2.66

The average specific gravity of the weak sandstone ranges from 2.54 to 2.68. Layer A in the Shihti Formation has a lower specific gravity than the above results probably because of distributions of kaolinite and coal in the layer.

Wave velocities

The experimental results regarding longitudinal wave and shear wave velocity measurements on the weak sandstones are shown in Table 5. Longitudinal wave velocity ranges from 0.48 km/sec to 4.84km/sec, while shear wave velocity from 0.32km/sec to 2.98km/sec. The results in Table 5 show that wave velocity in the Kweichulin Formation is higher than that in the Shihti Formation. It is the same in layers A and D of the Kweichulin Formation. Layers B and C have higher wave velocity.

Bieniawski (1984) found that longitudinal wave velocity of weak sandstones ranges from 1.1km/sec to 4.5km/sec. Yuan (1996) showed by experimental results that longitudinal wave velocity of the Kweichulin Formation ranges from 1.64km/sec to 2.51km/sec, whereas shear wave velocity from 1.30 km/sec to 2.00km/sec. The weak sandstones have lower wave velocity than the averages found in the earlier studies mentioned above.

Table 5. Results of longitudinal and shear wave measurements for various layer of the study area.

	Longitudinal wave (km/sec)	Shear wave (km/sec)
Shihti Formation (A layer)	0.92～2.01	0.50～1.139
Kweichulin Formation (B layer)	0.48～2.75	0.32～1.66
Kweichulin Formation (C layer)	2.00～4.84	1.29～2.98
Kweichulin Formation (D layer)	0.50～1.98	0.34～1.31

Uniaxial compressive strength

Uniaxial compressive strength of the 59 weak sandstone samples was tested with a standard compressive testing machine. Longitudinal and lateral strain measurements were obtained using LVDT (Linear Variable Differential Transformer). A few strain meters were destroyed during the testing procedure. Therefore, the total volume changes for those samples were derived from LVDT data and converted to a strain measurement.

Table 6 shows variation changes in uniaxial compressive strength of the weak sandstones. Compressive strength ranges from 2.57kg/cm^2 to 949.6kg/cm^2. Most of the strength values of the weak sandstone samples were under 200kg/cm^2. Axial strain is normally lower than 1% as measured by strain meter. The strain change measured from LVDT is 2-4 times higher than the results from the strain meter. A clear-ended effect occurred with all the samples during compressive tests. The associated lateral strain was less than 0.6%.

Uniaxial compressive strength in layer A of the Shihti Formation averages 21.94kg/cm^2. It is the lowest among the four layers of the study area. Axial strain is also the lowest at an average of 0.34%. Lateral strains average 0.20%. Higher uniaxial compressive strength in layer C of the Kweichulin Formation averages 166.61kg/cm^2.

Axial and lateral strains in layer C are only a little different compared to those in layer B. Uniaxial compressive strength in layer D of the Kweichulin Formation averages 40.94kg/cm^2. Axial strain is higher than that in the other four layers.

Table 6 also shows that layers B and C have higher uniaxial compressive strength than A and D. Axial and lateral strains for samples from the Kweichulin Formation are higher than those for samples from the Shihti Formation.

Uniaxial compressive strength for rocks is normally classified into 7 grades (ISRM, 1978), designated by the codes R0, R1, R2, R3, R4, R5 and R6. The uniaxial compressive strength for the sandstones of the study area falls within R0 to R2 categories. Approximately 69.2% of the experimental samples in layer A of the Shihti Formation belong to the R1 grade (i.e. very weak rock). The Kweichulin Formation samples were categorized as R2 grade. It was found that 61. 1% of layer B and 75% of layer C samples fell in this grade. Most samples from layer D of the Kweichulin Formation ranged between R0 to R2 (Tab. 7).

Slake durability

Thirty samples were tested for their slake durability. The test results were categorized using the Gamble's (1971) classification. The slake durability index was found to range from "very low" to "medium". Most samples in layer A of the Shihti Formation and in layer D of the Kweichulin Formation were found to be of "very low" grade. Layers B and C of the Kweichulin Formation were classified in the "low" to "medium" grades (Tab. 8).

RESULTS AND ANALYSIS

The above results are combined and analyzed below in terms of their uniaxial compressive strength.

Interrelationships of physical properties

The relationship of each of physical properties (water content, porosity and density) with uniaxial compressive strength is shown in Figure 3. Figure 3 (a) shows an inverse parabolic relationship between uniaxial compressive strength and water content. The relationships between the above properties for both the Kweichulin Formation and the Shihti Formation are not very significant (r=-0.48, -0.66). Atkinson (1982) points out that chemical reaction of water with SiO^{-2} in sandstone can form the ionic reaction [H-O-H]+[-Si-O-Si-] = [-Si-OH.HO-Si-]. This stress corrosion phenomenon produces a lower strength in uniaxial compression tests.

Table 6. Results of compressive strength tests and stress-strain measurements for various layers of study area.

	Uniaxial compressive strength (kg/cm^2)	Axial strain[1] (%)	Axial strain[2] (%)	Lateral strain[2] (%)
Shihti Formation (A layer)	2.57～52.43	0.37～2.1	0.13～0.77	0.07～0.52
Kweichulin Formation (B layer)	7.83～196.89	87～1.76	0.1～0.82	0.04～0.49
Kweichulin Formation (C layer)	146.38～193.74	1.13～1.43	0.25～0.67	0.09～0.47
Kweichulin Formation (D layer)	3.21～103.82	0.42～2.27	0.09～1.48	0.03～0.56

1: LVDT measurements

2: Strain gauge measurements

Table 7. The percentage of various grades of uniaxial compressive strength of weak sandstone in various layers of the study area.

	R0 Extremely weak rock	R1 Very weak rock	R2 Weak rock
Shihti Formation (A layer)	3 sets (23.1%)	9 sets (69.2%)	1 set (7.7%)
Kweichulin Formation (B layer)	1 set (5.6%)	6 sets (33.3%)	11 sets (61.1%)
Kweichulin Formation (C layer)	—	—	3 sets (75%)
Kweichulin Formation (D layer)	7 sets (29.2%)	9 sets (37.5%)	8 sets (33.3%)

Table 8. Results of slake durability tests for various layers of study area.

	First cycle index (km/sec)	Second cycle index (km/sec)	Grade
Shihti Formation (A layer)	10.6～84.3	0.5～59.0	Very low
Kweichulin Formation (B layer)	13.8～87.4	1.9～75.2	Low-medium
Kweichulin Formation (C layer)	8.1～78.3	1.3～65.5	Low-medium
Kweichulin Formation (D layer)	2.4～88.5	0.2～73.4	Very low

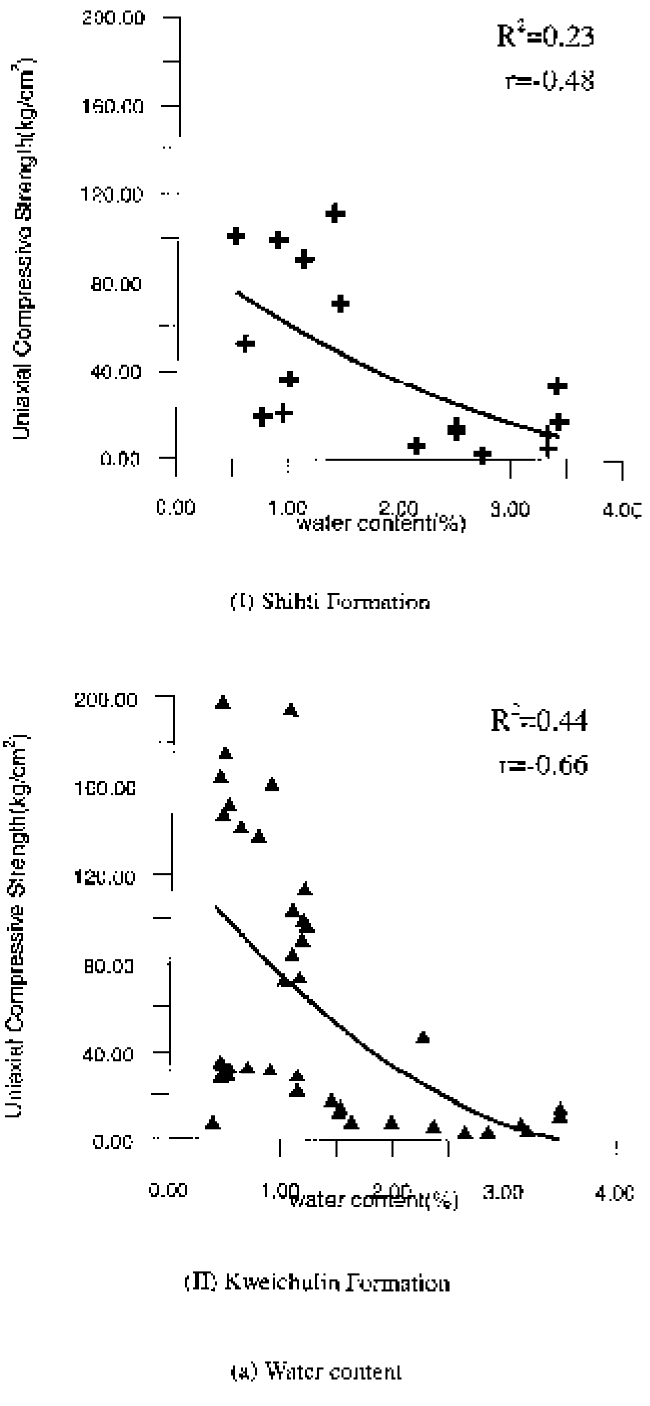

Figure 3a. The regression correction coefficient and the various linear relationships between uniaxial compressive strength and its physical properties (water content) in Shihti Formation and Kweichulin Formation.

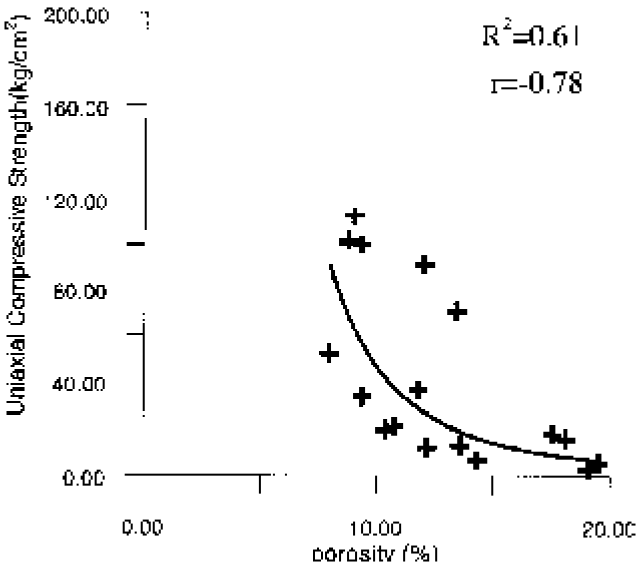

(I) Shihti Formation

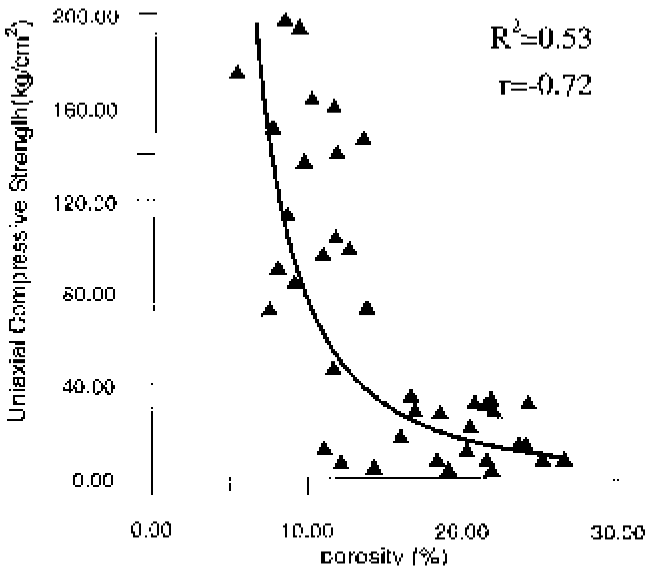

(II) Kweichulin Formation

(b) Porosity

Figure 3b. The regression correction coefficient and the various linear relationships between uniaxial compressive strength and its physical properties (porosity) in Shihti Formation and Kweichulin Formation. (Cont'd).

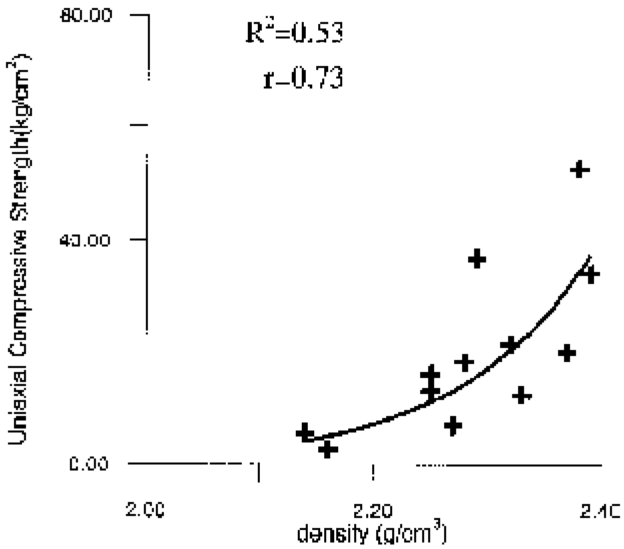

(I) Shihti Formation

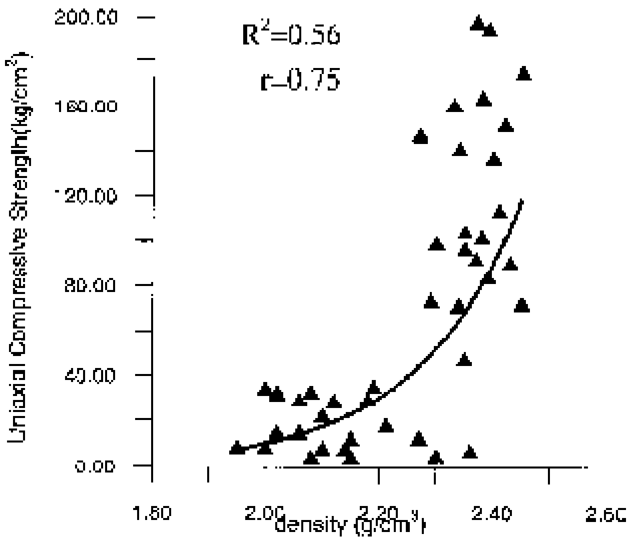

(II) Kweichulin Formation

(c) Density

Figure 3c. The regression correction coefficient and the various linear relationships between uniaxial compressive strength and its physical properties (density) in Shihti Formation and Kweichulin Formation. (Cont'd).

When water content of the weak sandstone samples is under 1% in this study, uniaxial compressive strength decreases rapidly with increasing water content. However, the decrease in uniaxial compressive strength is much less for water content values in excess of 1%. These results also indicate that pore water pressure did not affect uniaxial compressive strength. This summary is congruent with the results of Hawkins and McConnell (1992).

Figure 3 (b) shows increased significance of an inverse parabolic relationship between uniaxial compressive strength and porosity (significance level: r=-0.78, -0.72). Uniaxial compressive strength decreases as porosity increases. When porosity is under 15%, the uniaxial compressive strength rapidly increases as porosity decreases. These results reveal that porosity can be a major factor in those voids and thereby in reducing rock strength.

Uniaxial compressive strength also increases as density increases. Figure 3 (c) shows that a positive parabolic relationship between uniaxial compressive strength and density is also quite significant (r=0.73, 0.75). When density is more than 2.3g/cm^3, uniaxial compressive strength is dramatically higher. This trend is almost exactly opposite the downward trend observed regarding density and porosity.

The above results show that denser weak sandstone has a higher uniaxial compressive strength. When the porosity is lower than 15% or the density is higher than 2.3g/cm^3, uniaxial compressive strength of the weak sandstone increases.

Mineral composition relationships

Comparison of uniaxial compressive strength, wave velocity and slake durability measurements with mineral composition is shown in Figure 4. Figure 4 (a) shows an inverse linear relationship between quartz content and uniaxial compressive strength. There is no clear trend indicated and no statistical significance found in the Shihti Formation. The Kweichulin Formation also exhibits no significant relationship (r=-0.48).

Figure 4 (b) shows a positive linear relationship between the proportion of matrix and uniaxial compressive strength. There is also no clear trend indicating statistical significance found in the Shihti Formation. The Kweichulin Formation also showed no significant relationship (r=0.43). Uniaxial compressive strength and proportion of detritus data are combined in Figure 4 (c). The correlation coefficient r remains very low at -0.31 and 0.5.

The Kweichulin weak sandstone shows a positive relationship between uniaxial compressive strength with matrix and detritus content. In the Shihti Formation, mineral (quartz and matrix) contents seem to have no clear relationship or trend with regard to uniaxial compressive strength.

Relation in wave velocity

Figure 5 shows a positive linear relationship between uniaxial compressive strength and wave velocities (longitudinal wave and shear wave) of the weak sandstone. The relationship between the two properties for both the Kweichulin and Shihti Formations is quite significant (r=0.89, 0.85 and 0.84, 0.87 respectively).

These results demonstrate a positive trend such that when wave velocity is higher, uniaxial compressive strength is higher. The correlation coefficient (r) between longitudinal wave and uniaxial compressive strength is 0.75. The correlation coefficient (r) between shear wave and uniaxial compressive strength is 0.79. The correlation coefficient (r) between both longitudinal wave and shear wave is 0.99. They display a positive linear correlation. The regression analysis formulae is $Vs = 0.62 \times Vp$.

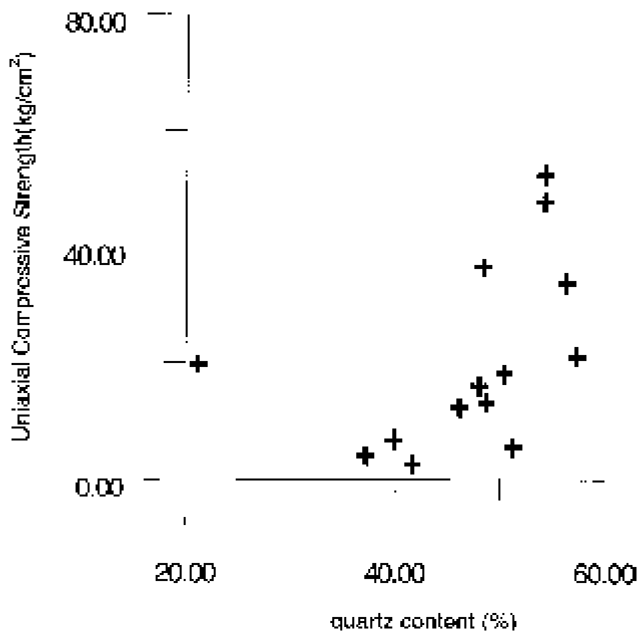

(I) Shihti Formation

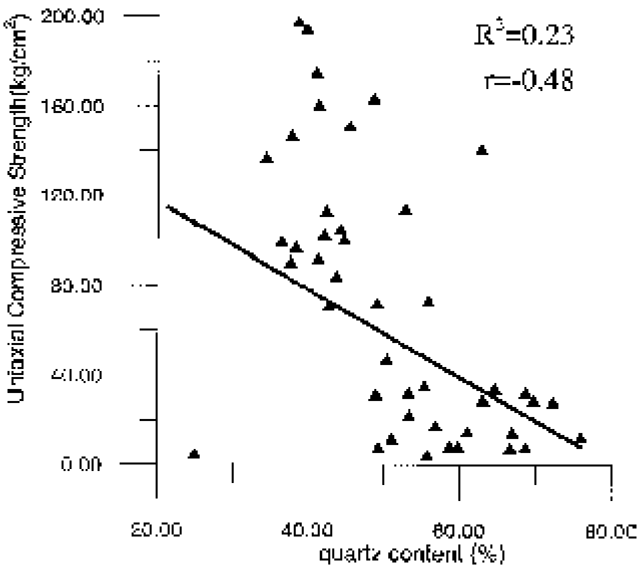

(II) Kweichulin Formation

(a) Quartz content

Figure 4a. The regression correction coefficient and the various linear relationships between uniaxial compressive strength and its minerals composition (quartz content) in Shihti Formation and Kweichulin Formation.

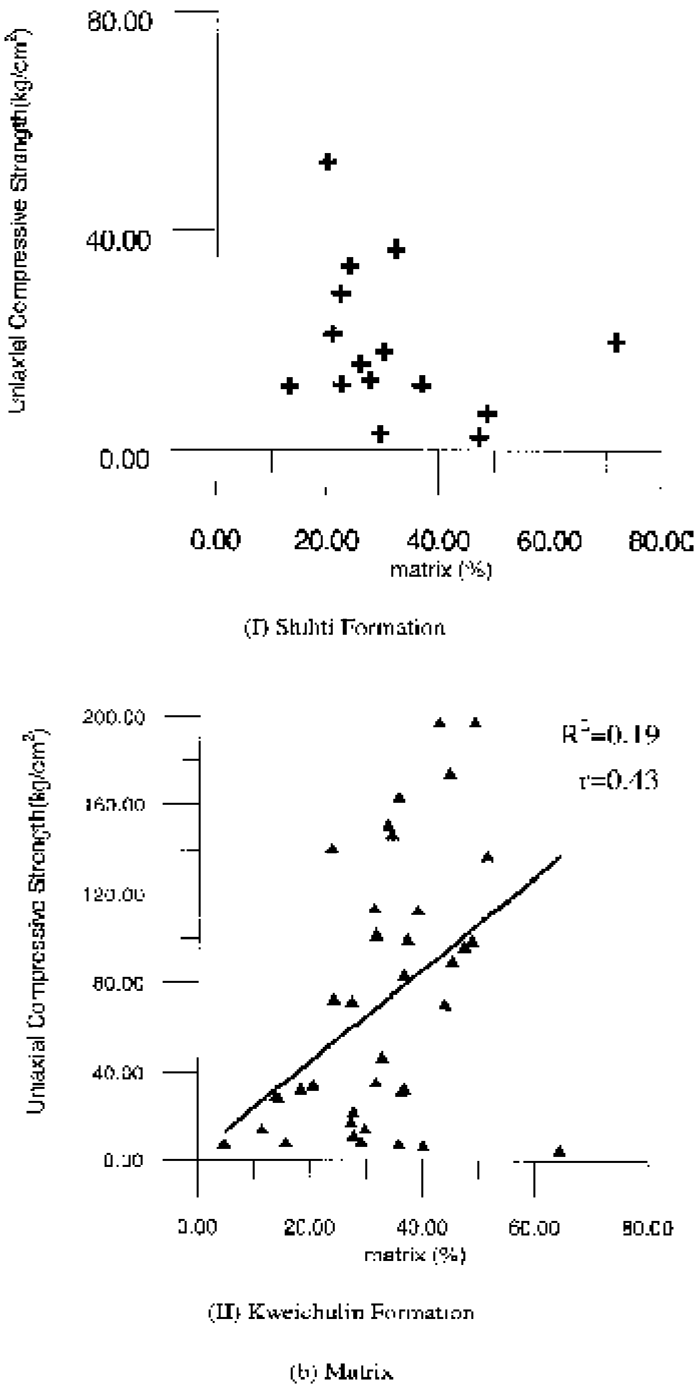

(I) Shihti Formation

(II) Kweichulin Formation

(b) Matrix

Figure 4b. The regression correction coefficient and the various linear relationships between uniaxial compressive strength and its minerals composition (matrix) in Shihti Formation and Kweichulin Formation.(Cont' d).

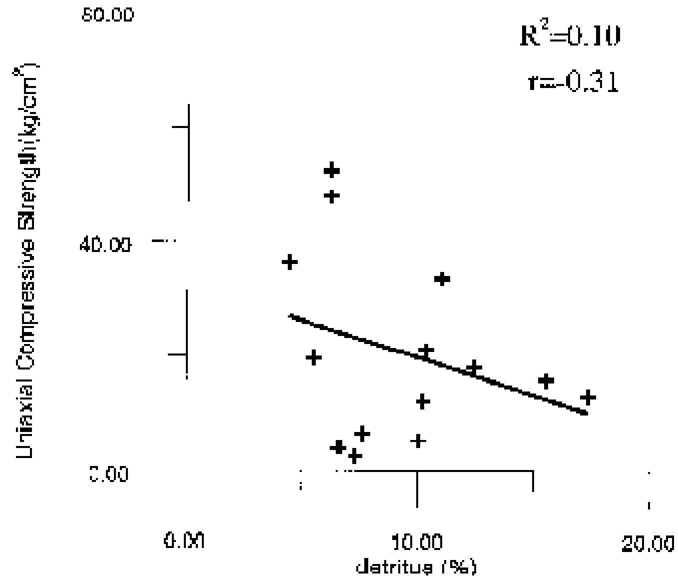

(I) Shihti Formation

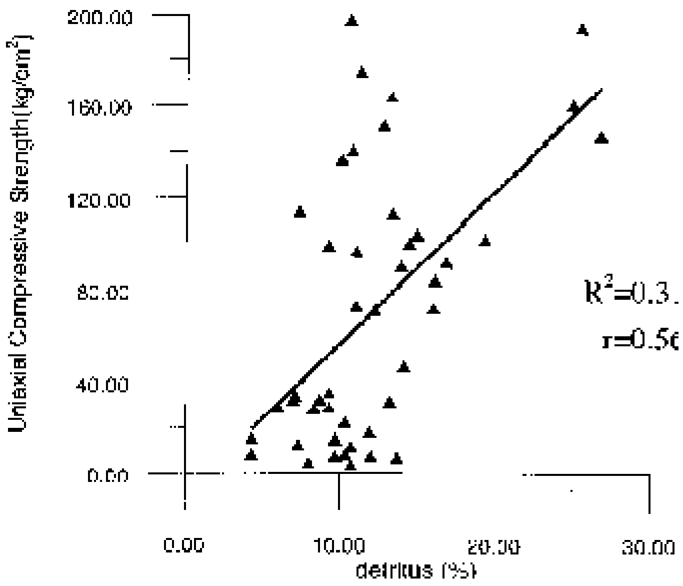

(II) Kweichulin Formation

(c) Detritus

Figure 4c. The regression correction coefficient and the various linear relationships between uniaxial compressive strength and its minerals composition (detritus) in Shihti Formation and Kweichulin Formation. (Cont'd).

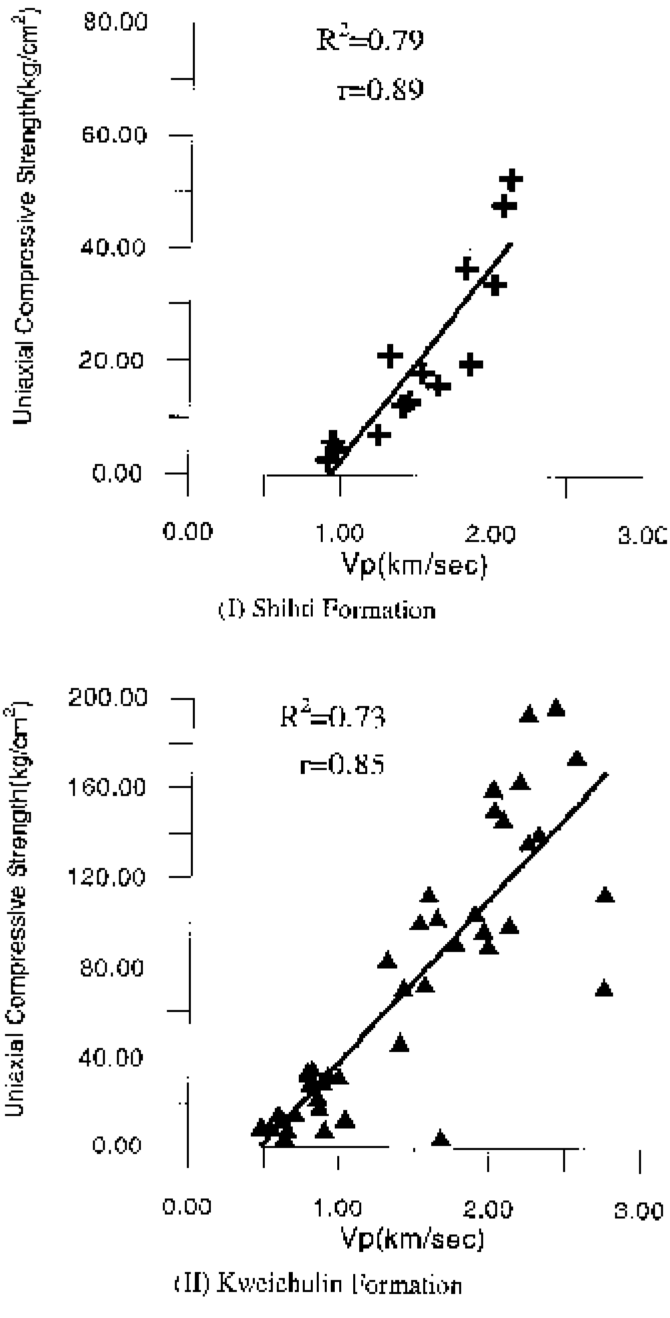

(a) Longitudinal wave

Figure 5a. The regression correction coefficient and the various linear relationships between uniaxial compressive strength and its longitudinal (Vp) and shear (Vs) wave in Shihti Formation and Kweichulin Formation.

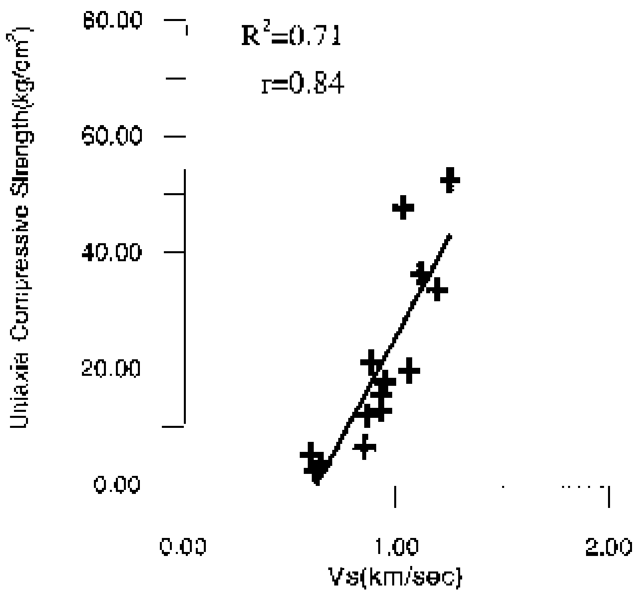

(I) Shihti Formation

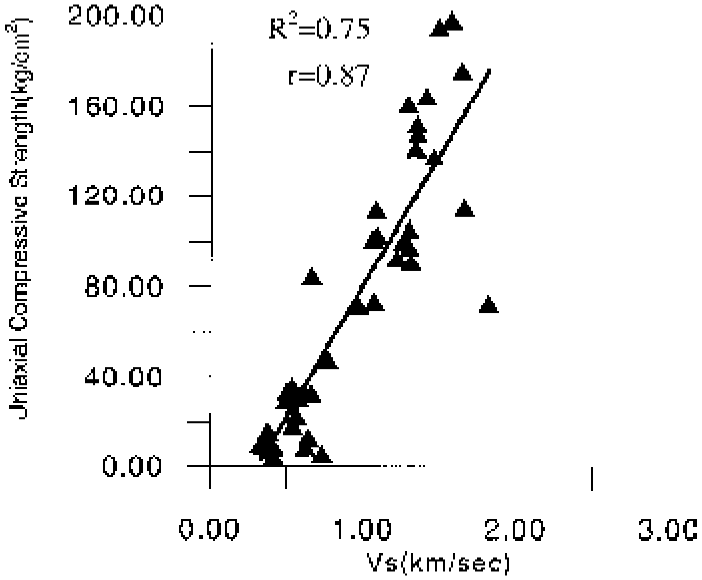

(II) Kweichulin Formation

(b) Shear wave

Figure 5b. The regression correction coefficient and the various linear relationships between uniaxial compressive strength and its longitudinal (Vp) and shear (Vs) wave in Shihti Formation and Kweichulin Formation. (Cont'd).

Figure 6 shows different relationships between wave velocity and physical properties. There is a weak relationship between wave velocity and water content, and a strong relationship of wave velocity and porosity with density. The correlation coefficients (r) of porosity (Figures 6 (c) and (d)) and density (Figures 6 (e) and (f)) are all quite significant (porosity: r = -0.80, -0.81; density: r = 0.85, 0.86).

Figure 7 shows the relationships between wave velocity and mineral contents. The data are too random to be statistically significant.

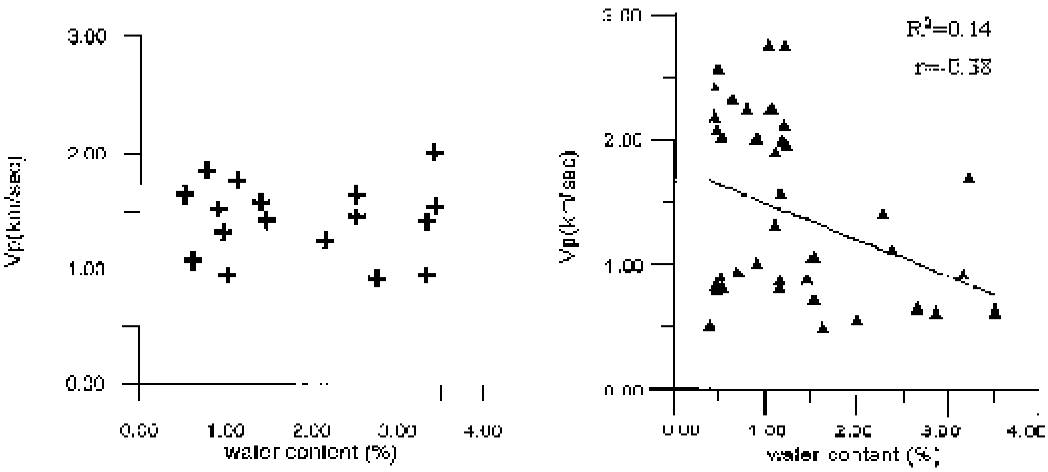

(I) Shihti Formation (II) Kweichulin Formation

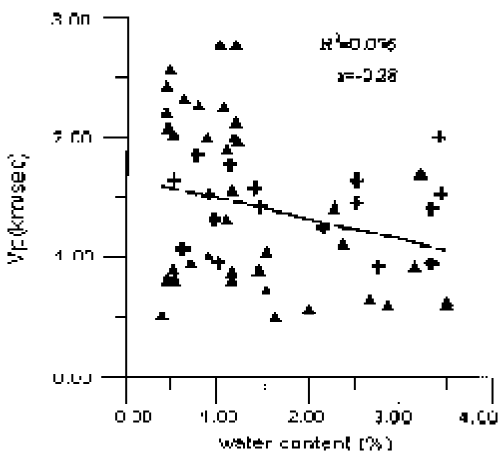

(a) Water content

Figure 6a. The regression correction coefficient and the various linear relationships between wave velocity (longitudinal wave, Vp) and physical properties (water content) in Shihti Formation and Kweichulin Formation.

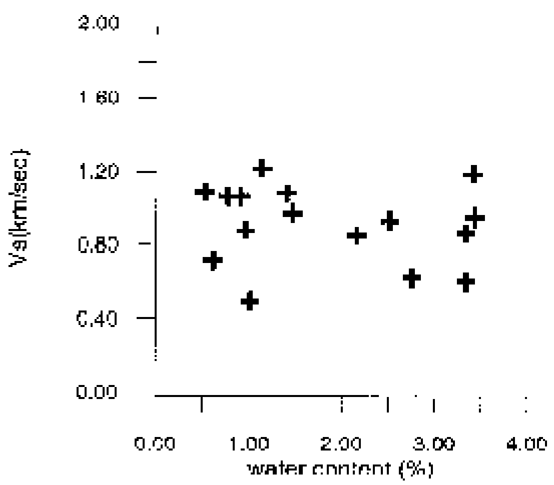

(I) Shihti Formation

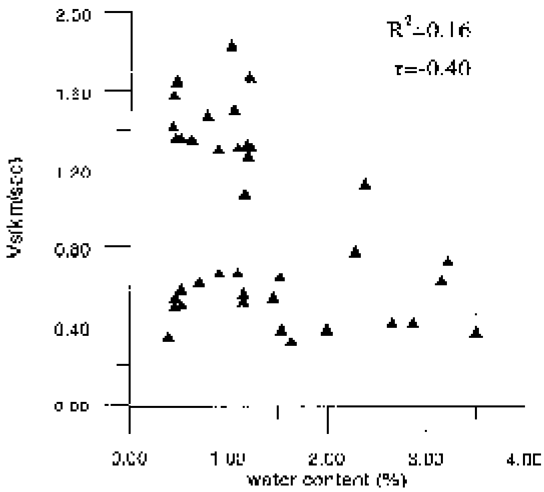

(II) Kweichulin Formation

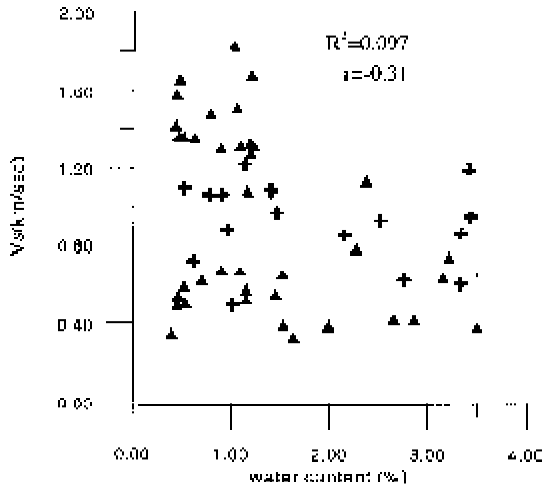

(b) Water content

Figure 6b. The regression correction coefficient and the various linear relationships between wave velocity (shear wave, Vs) and physical properties (water content) in Shihti Formation and Kweichulin Formation. (Cont'd).

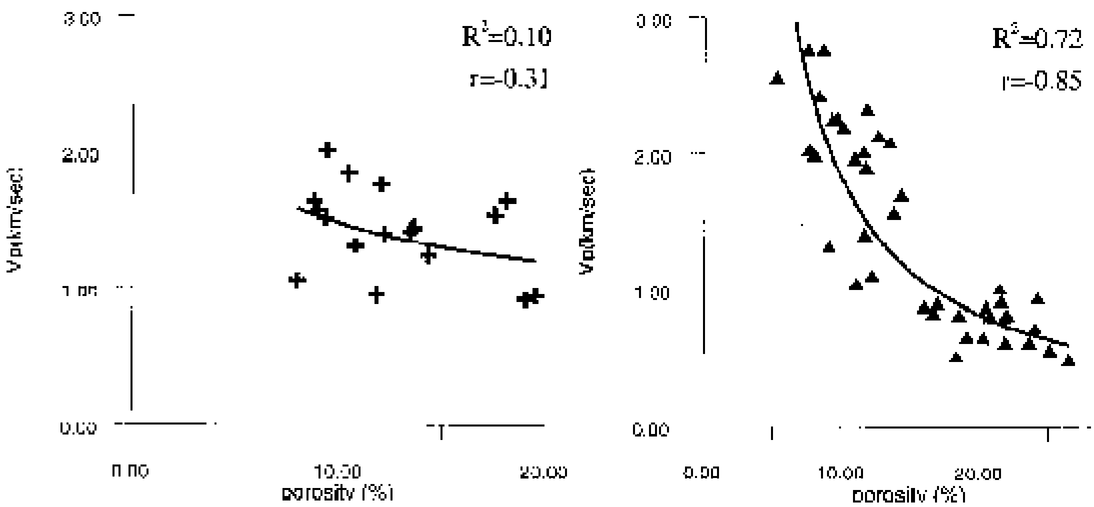

(I) Shihti Formation (II) Kweichulin Formation

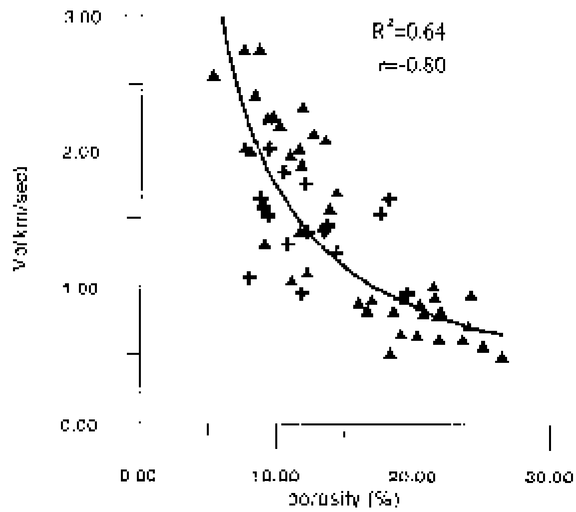

(c) Porosity

Figure 6c. The regression correction coefficient and the various linear relationships between wave velocity (longitudinal wave, Vp) and physical properties (porosity) in Shihti Formation and Kweichulin Formation. (Cont' d).

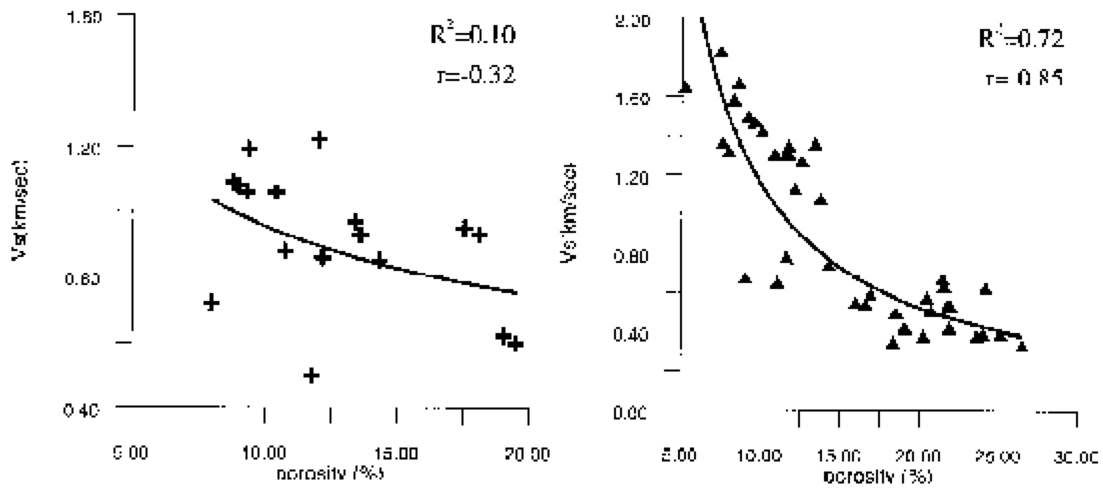

(I) Shihti Formation (II) Kweichulin Formation

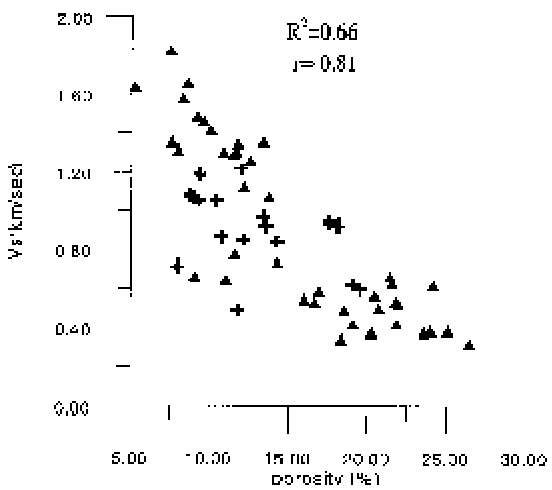

(d) Porosity

Figure 6d. The regression correction coefficient and the various linear relationships between wave velocity (shear wave, Vs) and physical properties (porosity) in Shihti Formation and Kweichulin Fomation.(Cont' d).

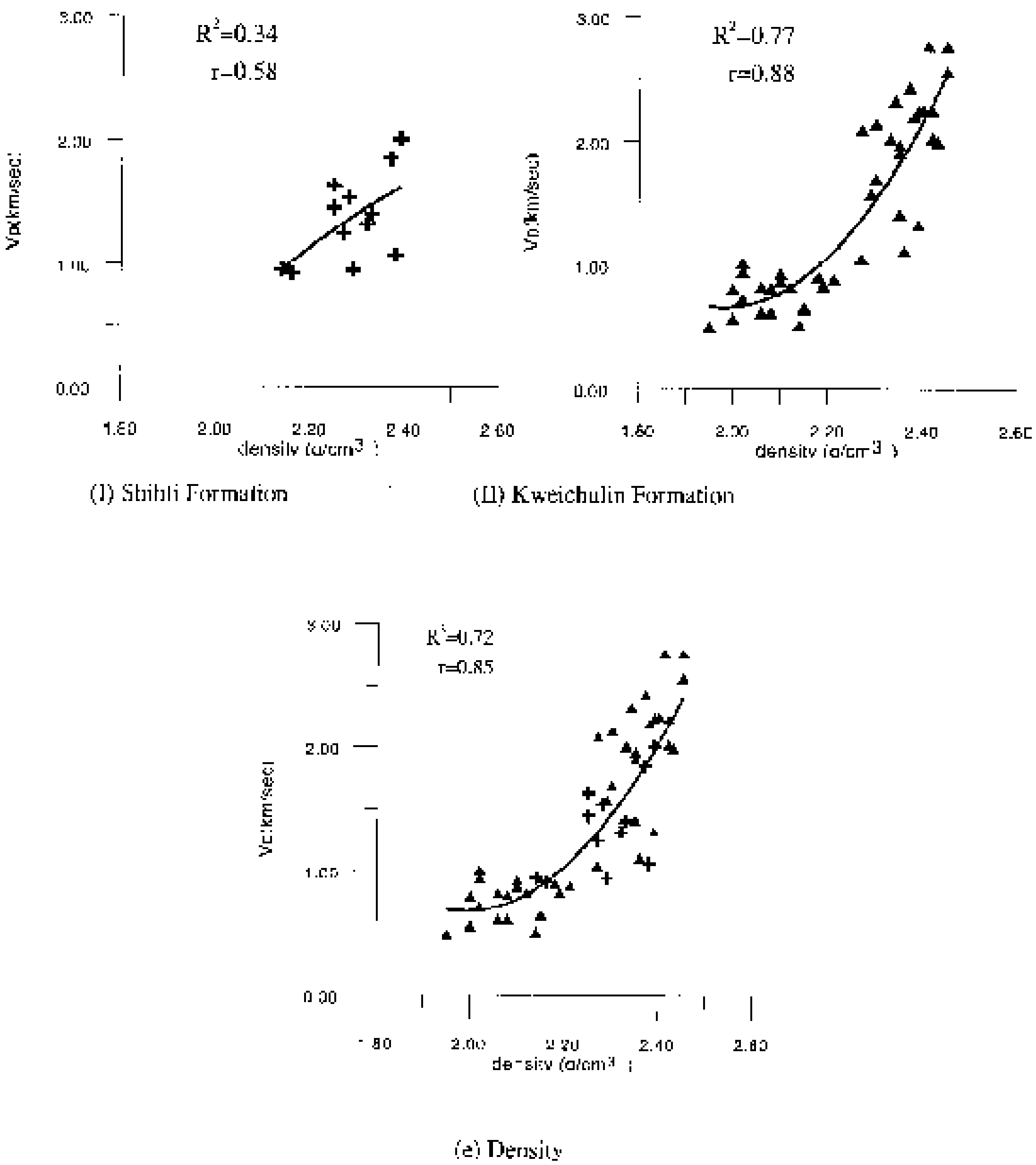

Figure 6e. The regression correction coefficient and the various linear relationships between wave velocity (longitudinal wave, Vp) and physical properties (density) in Shihti Formation and Kweichulin Formation.(Cont'd).

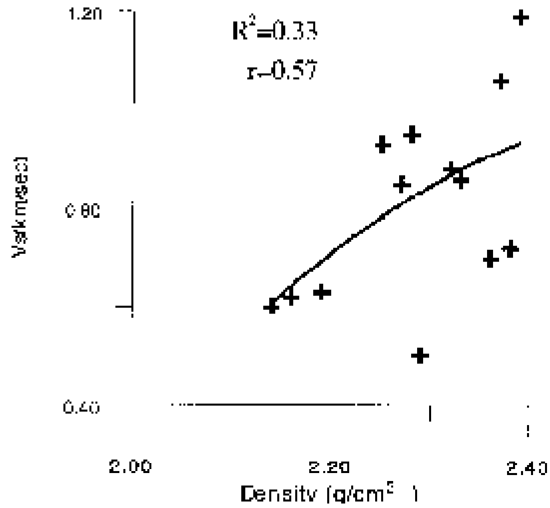

(I) Shihti Formation

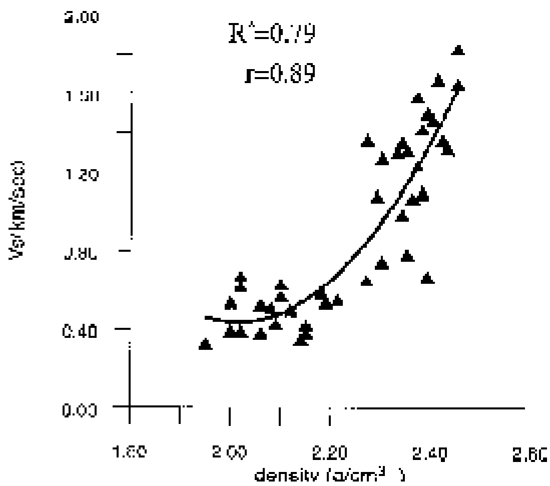

(II) Kweichulin Formation

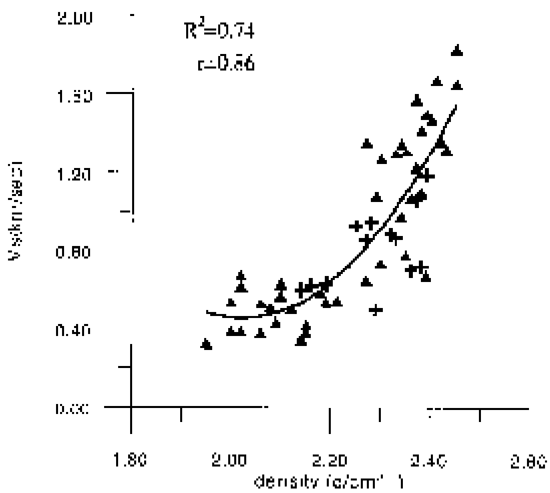

(f) Density

Figure 6f. The regression correction coefficient and the various linear relationships between wave velocity (shear wave, Vs) and physical properties (density) in Shihti Formation and Kweichulin Formation. (Cont'd).

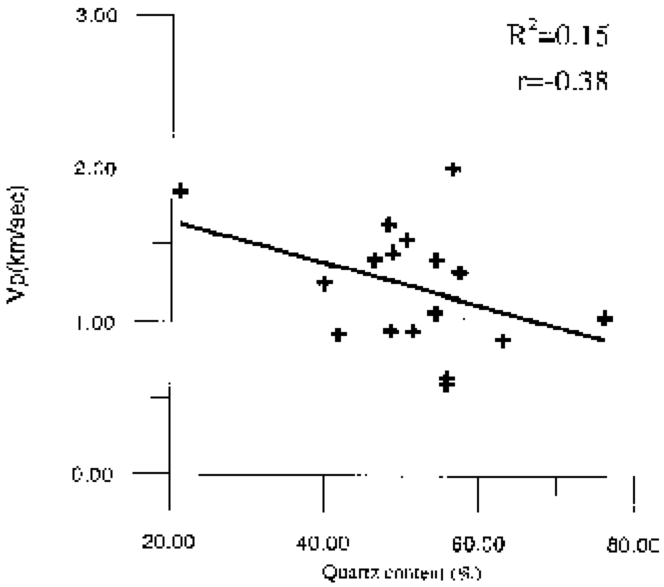

(I) Shihti Formation

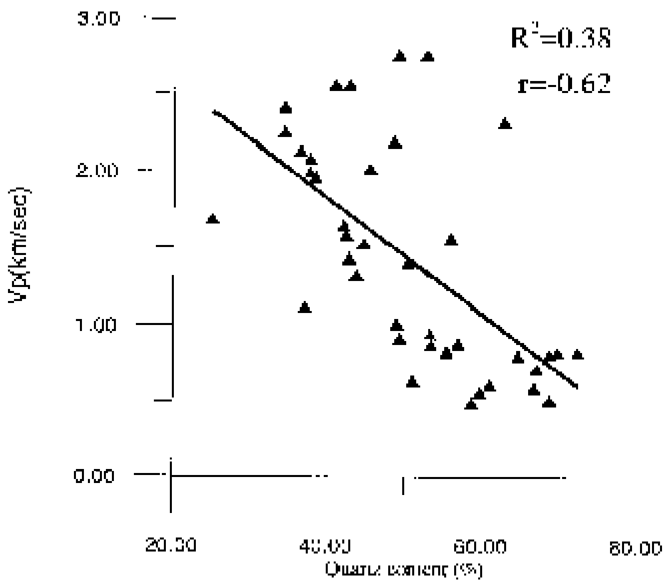

(II) Kweichulin Formation

(a) Quartz content

Figure 7a. The regression correction coefficient and the various linear relationships between wave velocity (longitudinal wave, Vp) and its mineral composition (quartz content) in Shihti Formation and Kweichulin Formation.

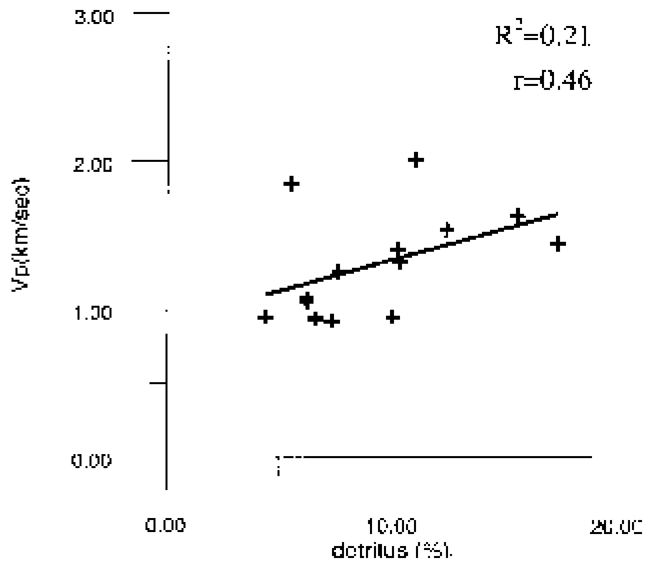

(I) Shihli Formation

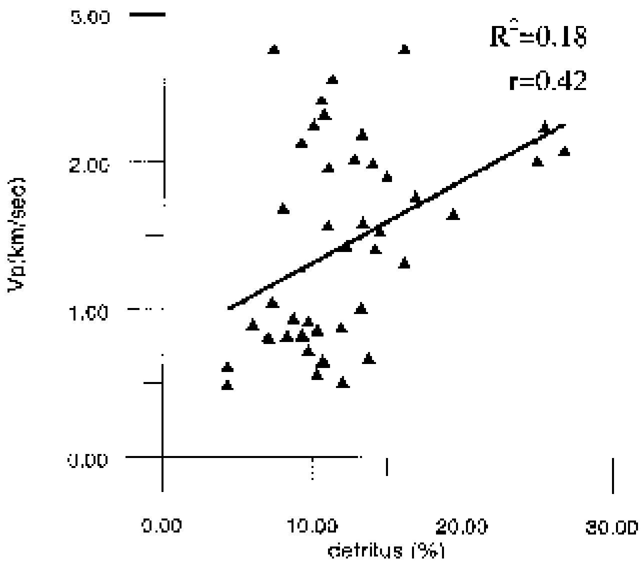

(II) Kweichulin Formation

(b) Detritus

Figure 7b. The regression correction coefficient and the various linear relationships between wave velocity (longitudinal wave, Vp) and its mineral composition (detritus) in Shihti Formation and Kweichulin Formation. (Cont'd).

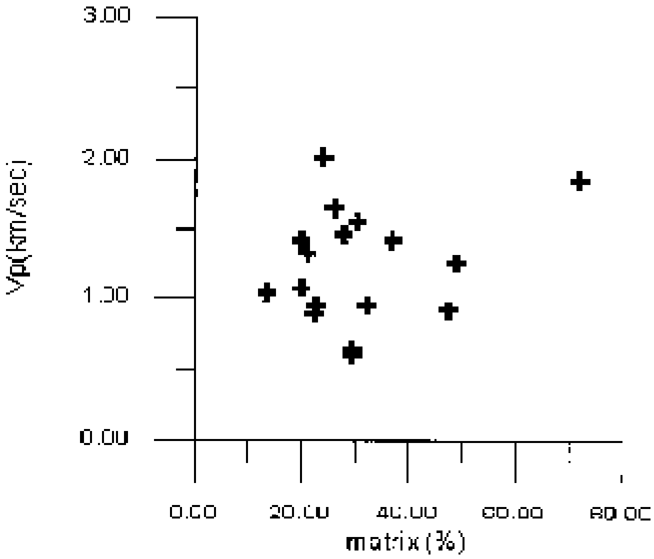

(I) Shihti Formation

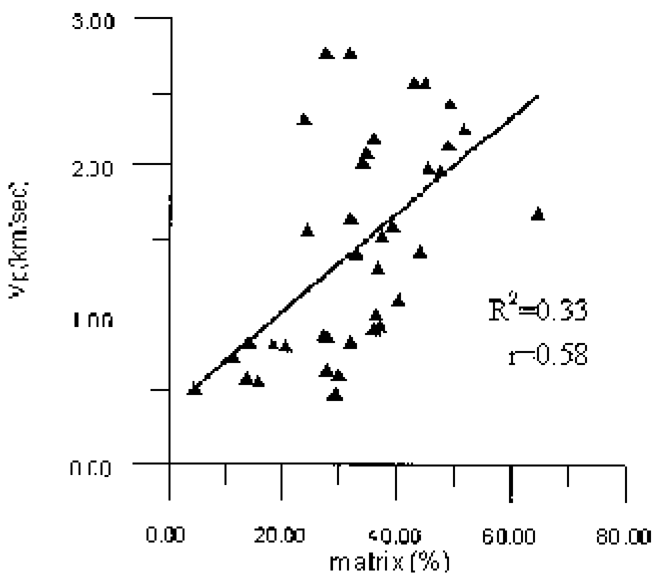

(II) Kweichulin Formation

(c) Matrix

Figure 7c. The regression correction coefficient and the various linear relationships between wave velocity (longitudinal wave, Vp) and its mineral composition (matrix) in Shihti Formation and Kweichulin Formation. (Cont'd).

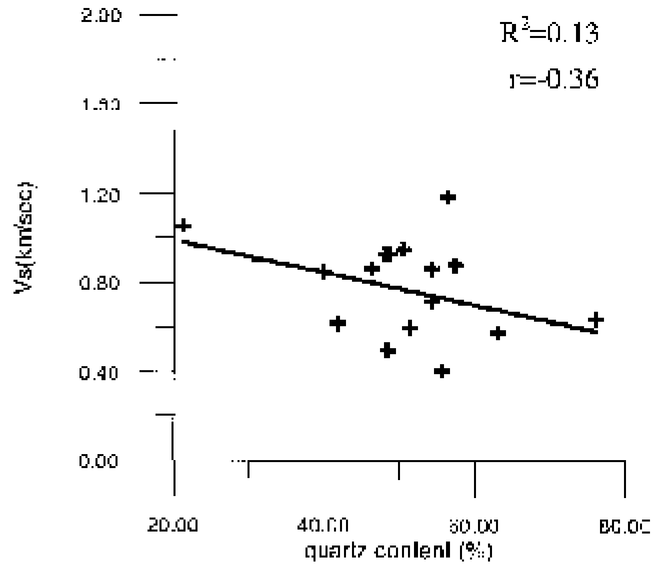

(I) Shihti Formation

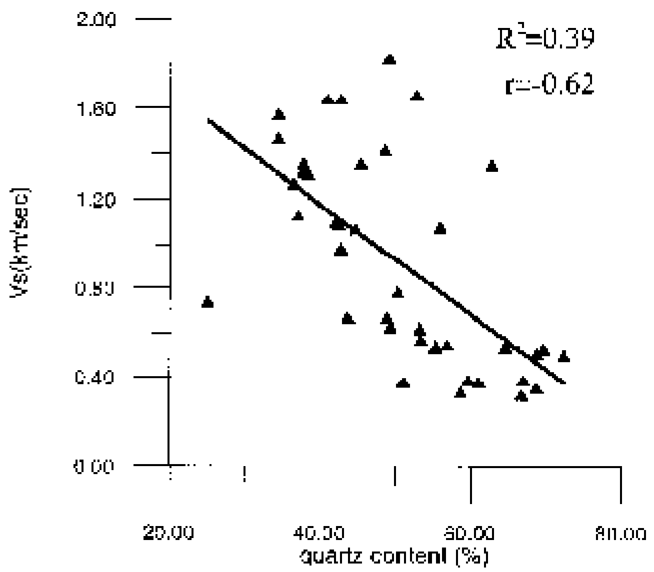

(II) Kweichulin Formation

(d) Quartz content

Figure 7d. The regression correction coefficient and the various linear relationships between wave velocity (shear wave, Vs) and its mineral composition (quartz content) in Shihti Formation and Kweichulin Formation. (Cont'd).

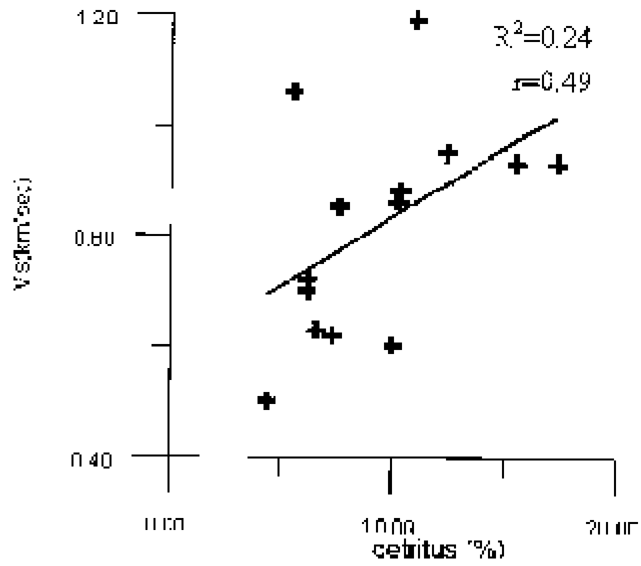

(I) Shihti Formation

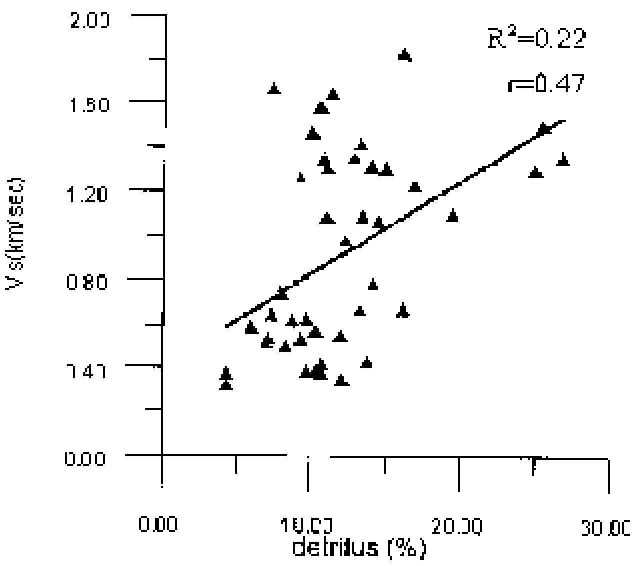

(II) Kweichulin Formation

(e) Detritus

Figure 7e. The regression correction coefficient and the various linear relationships between wave velocity (shear wave, Vs) and its mineral composition (detritus) in Shihti Formation and Kweichulin Fomation.

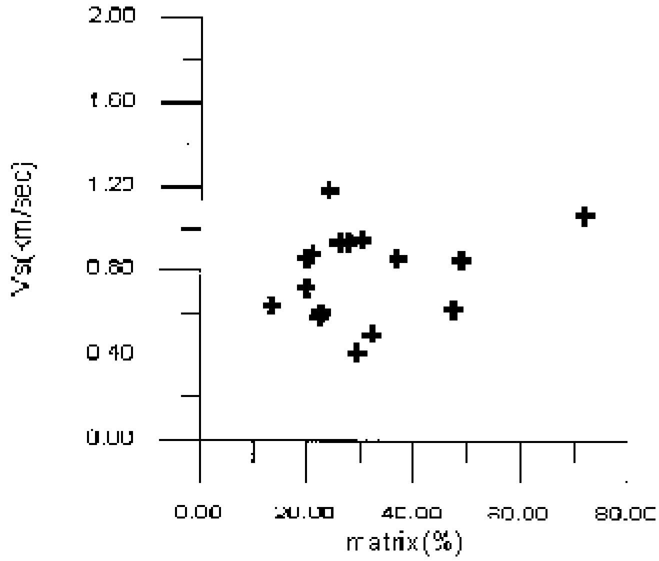

(I) Shihti Formation

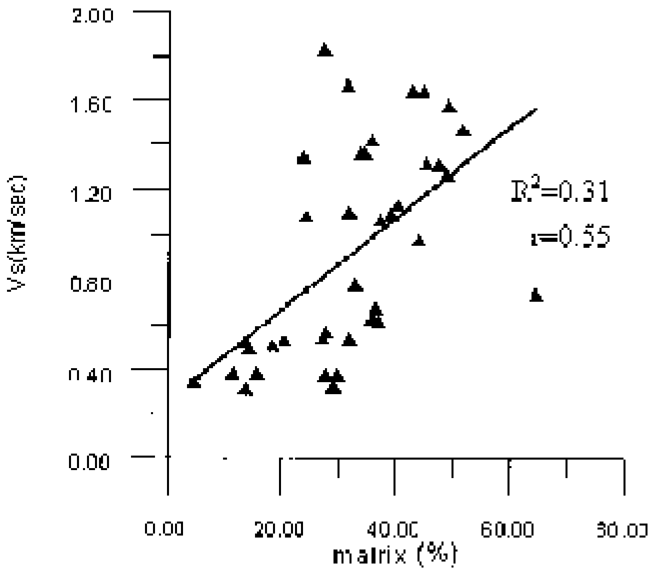

(II) Kweichulin Formation

(f) Matrix

Figure 7f. The regression correction coefficient and the various linear relationships between wave velocity (shear wave, Vs) and its mineral composition (matrix)in Shihti Fomation and Kweichulin Formation. (Cont'd).

Relationship of slake durability

Figure 8 shows a positive linear relationship between first cycle and second cycle slake durability index values and uniaxial compressive strength. The first cycle index of slake durability yields a more significant correlation coefficient r=0.73 only in the Kweichulin Formation (Fig. 8 (a)). The second cycle index of slake durability (Fig. 8 (b)) shows low significance (r=0.68). The results of slake durability (first cycle index and second cycle index) comparisons with respect to mineral contents are still not very clear (Figures 9 and 10). This means that the index of slake durability does not have a very good relationship with uniaxial compressive strength and mineral content.

CONCLUSIONS

1. The major constituent of the matrix of the rocks in the study area is clay mineral. The types of clay minerals in the Kweichulin and the Shihti Formations are quite different. The former contains only rare amounts of smectite and chorite but is rich in kaolinite whereas the latter contains more illite and chorite.

2. When the weak sandstone is denser, uniaxial compressive strength is higher.

3. The test results point out that when porosity is lower than 15% or density is over 2.3 g/m^3, decreasing porosity will affect uniaxial compressive strength of the weak sandstone.

4. The experimental results show a positive trend between uniaxial compressive strength and contents of matrix and detritus. However, uniaxial compressive strength shows only a minor increase with increasing quartz content. This means that mineral composition cannot be considered as a major factor affecting uniaxial compressive strength and wave velocity of the weak sandstone studied.

5 The regression analysis shows that wave velocity has a positive linear trend with uniaxial compressive strength.

6 The results show that the slake durability index does not have a good relationship with uniaxial compressive strength and mineral contents.

ACKNOWLEDGMENTS

The authors would like to thank Prof. L. A. Lee, Institute of Statistic Analysis, Academy Sinica, and Prof. T. H. Huang, Department of Civil Engineering, National Taiwan University, Prof. C. L. Pan, Ministry of Economic Affairs, Dr. H. C. Lee, Department of Civil Engineering, Chungyun University, Dr. C. C. Chen, Sinotech Engineering Consultants, and Dr. Del Dobyns, Ming Chuan College for their constructive comments. The funding came from the National Science Council (NSC 86-2116-M-002-016) of ROC.

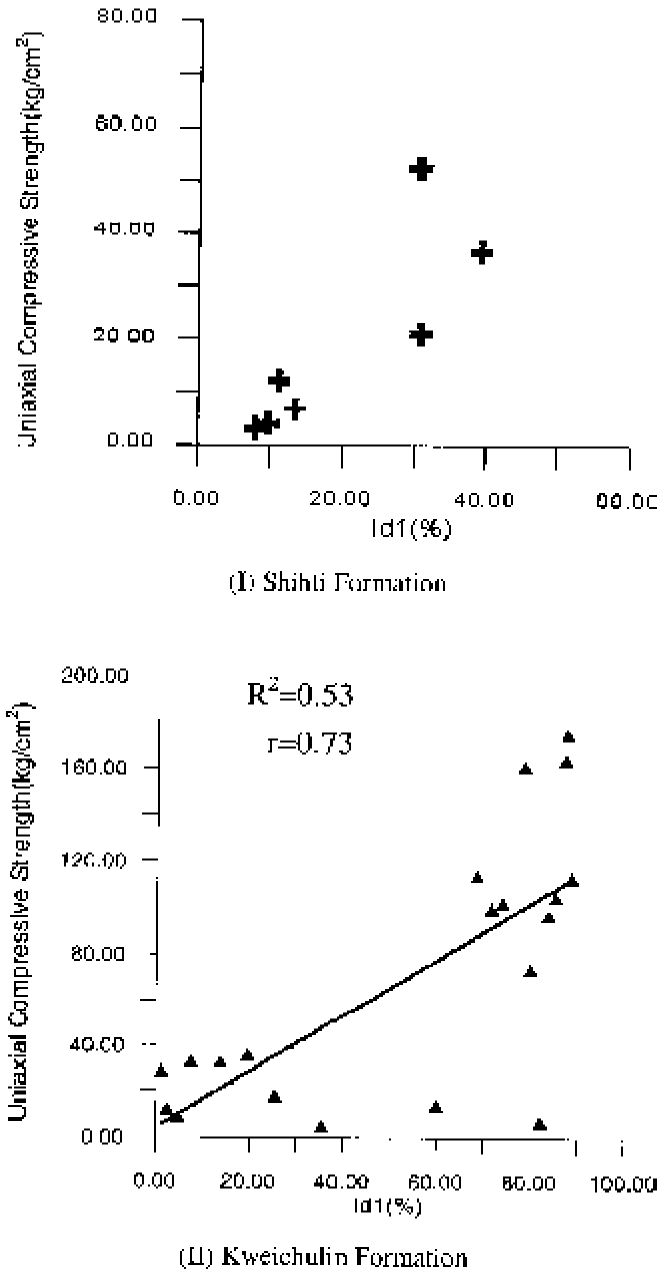

(a) First cycle index

Figure 8a. The regression correction coefficient and the various linear relationships between uniaxial compressive strength and slaking durability (first cycle index, Id1) in Shihti Formation and Kweichulin Fomation.

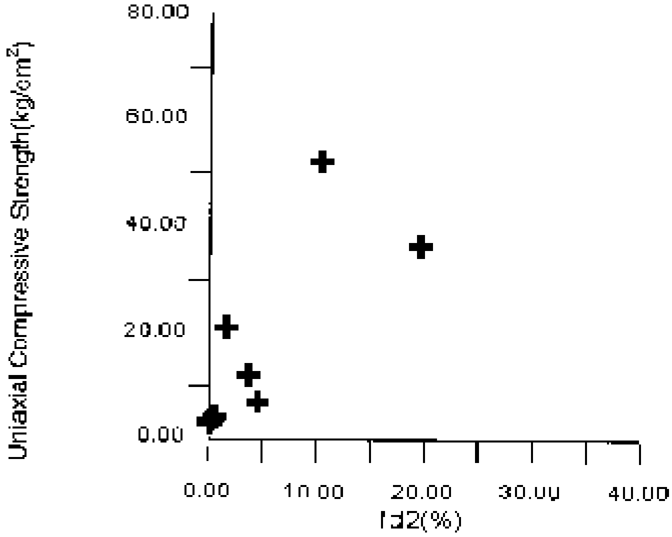

(I) Shihti Formation

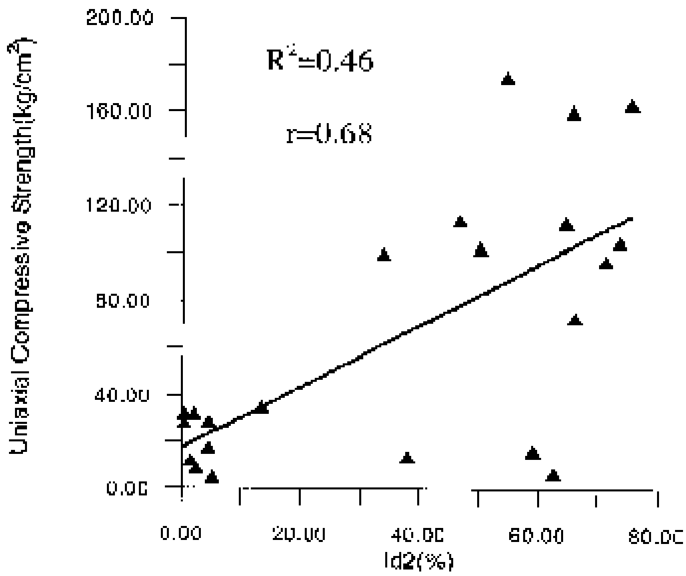

(II) Kweichulin Formation

(b) Second cycle index

Figure 8b. The regression correction coefficient and the various linear relationships between uniaxial compressive strength and slaking durability (second cycle index, Id2) in Shihti Formation and Kweichulin Formation. (Cont'd).

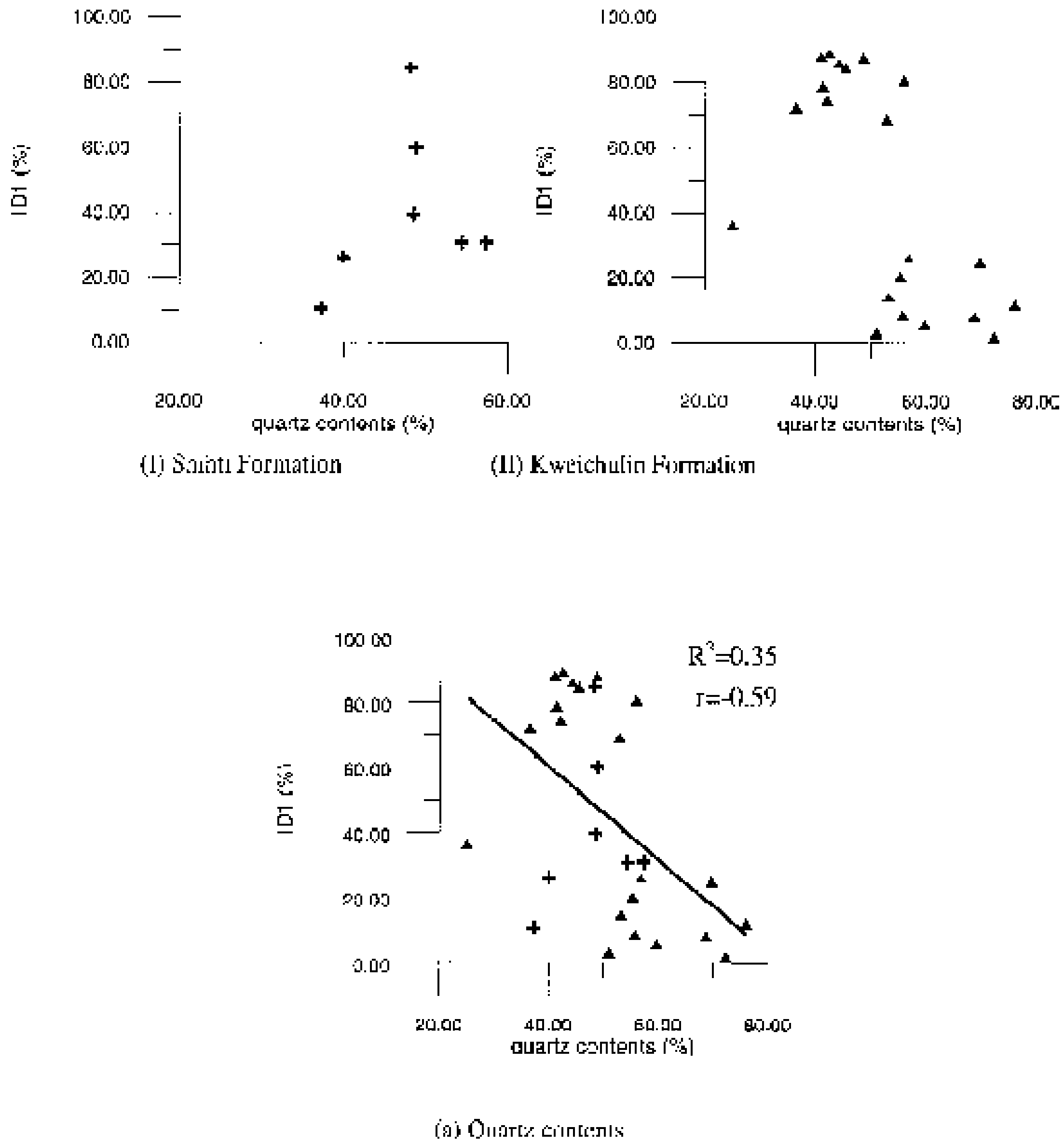

Figure 9a. The regression correction coefficient and the various linear relationships between slaking durability (first cycle index,Id1) and mineral composition (quartz content) in Shihti Formation and KweichulinFormation.

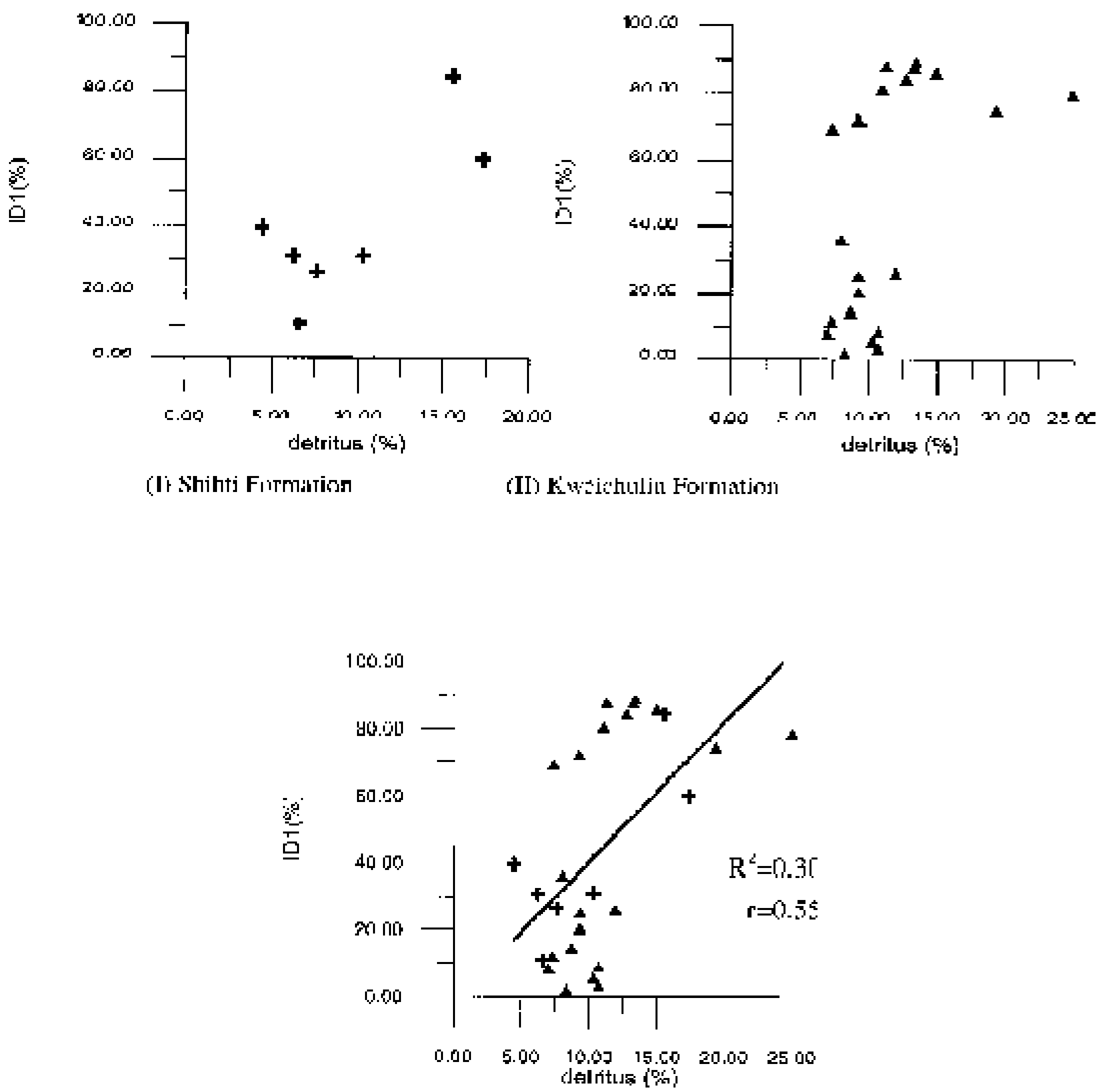

Figure 9b. The regression correction coefficient and the various linear relationships between slaking durability (first cycle index, Id1) and minerial composition (detritus) in Shihti Formation and Kweichulin Formation. (Cont'd).

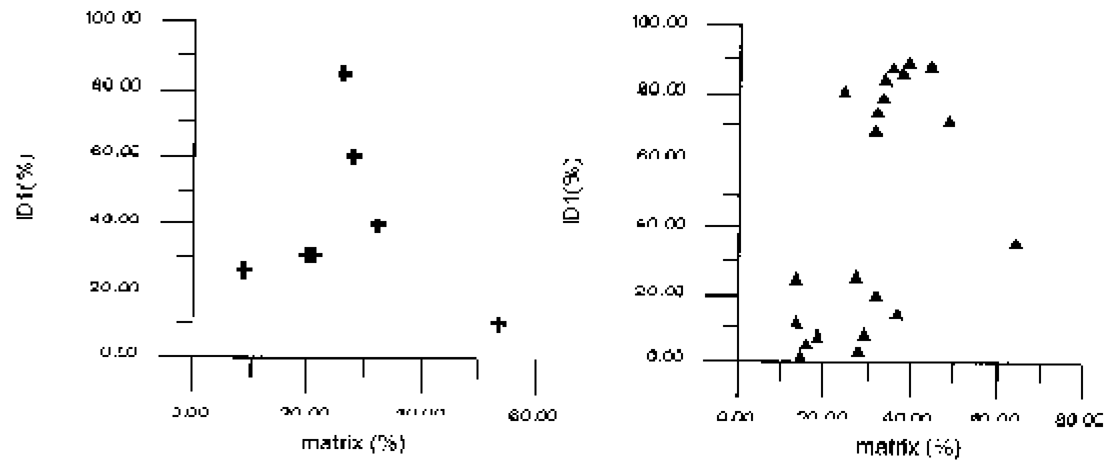

(I) Shihti Formation (II) Kweichulin Formation

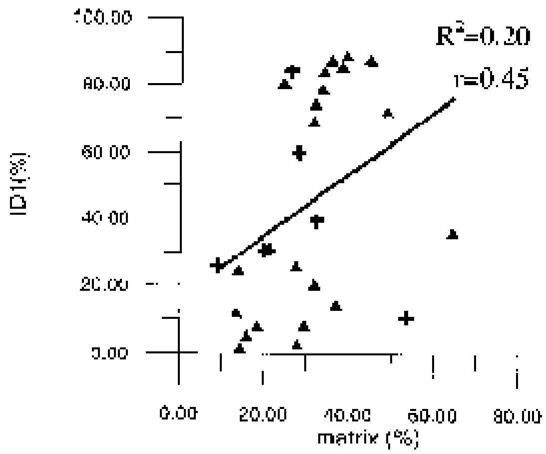

(c) matrix

Figure 9c. The regression correction coefficient and the various linear relationships between slaking durability (first cycle index, Id1) and mineral composition (matrix) in Shihti Formation and Kweichulin Formation. (Cont'd).

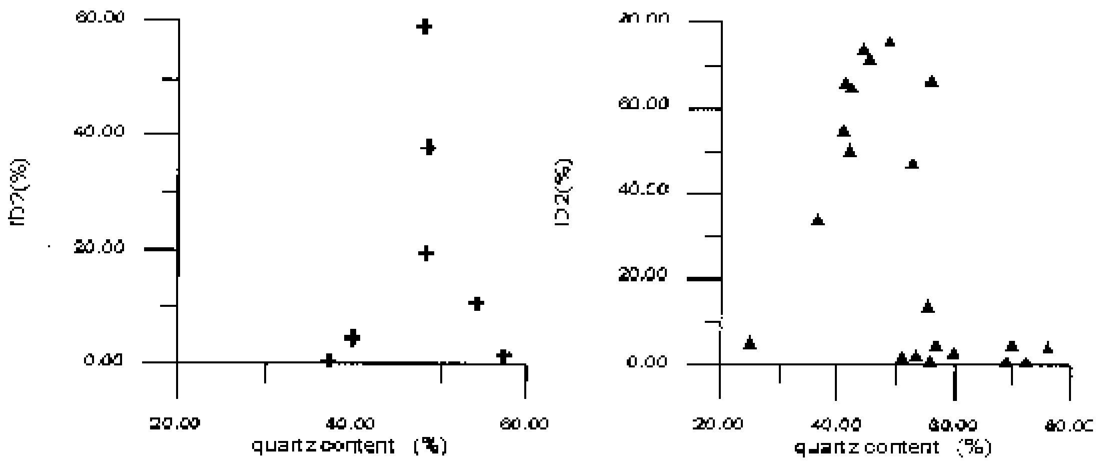

(I) Shihti Formation (II) Kweichulin Formation

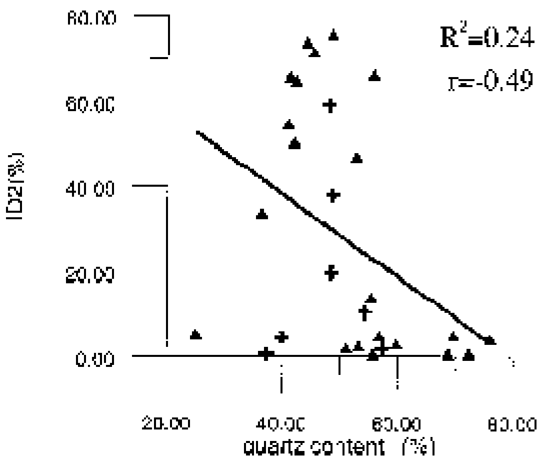

(a) Quartz content

Figure 10a. The regression correction coefficient and the various linear relationships between slaking durability (second cycle index, Id2) and mineral composition (quartz content) in Shihti Formation and Kweichulin Formation.

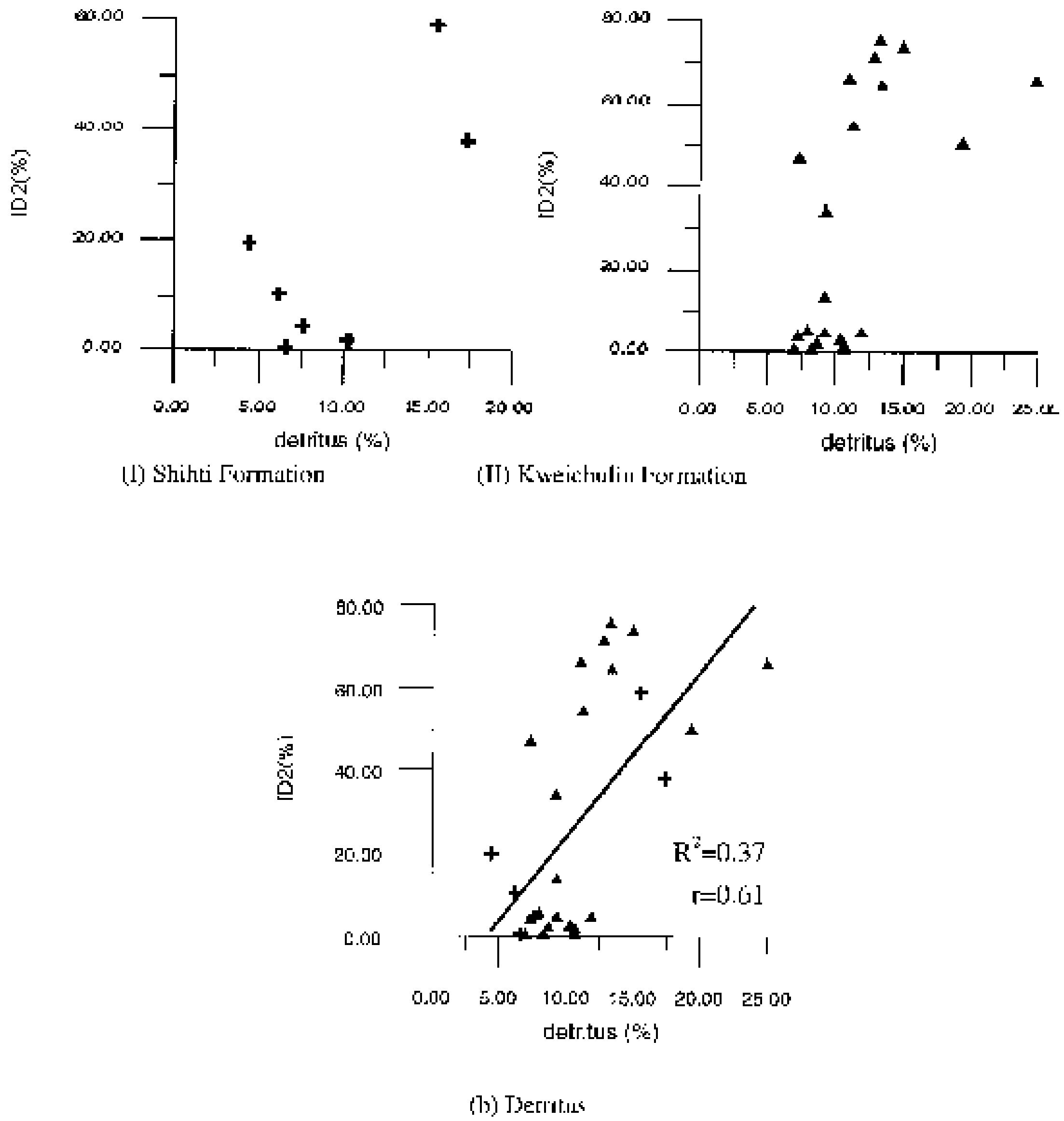

Figure 10b. The regression correction coefficient and the various linear relationships between slaking durability (second cycle index, Id2) and mineral composition (detritus) in Shihti Formation and Kweichulin Formation. (Cont'd).

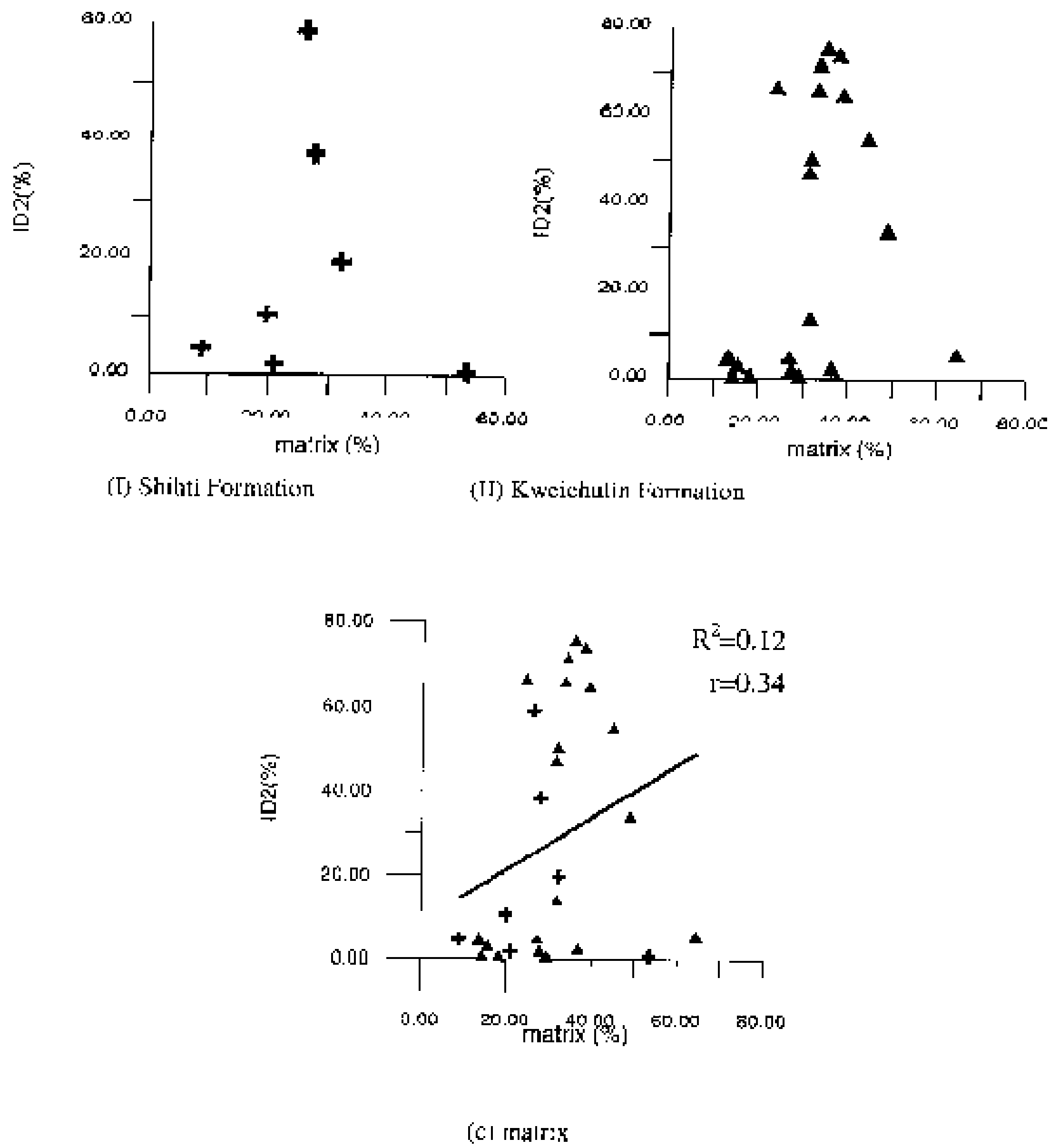

Figure 10c. The regression correction coefficient and the various linear relationships between slaking durability (second cycle index, Id2) and mineral (matrix) in Shihti Formation and Kweichulin Formation. (Cont'd).

REFERENCES

Atkinson, B. K, (1982) Subcritical crack propagation in rocks: theory, experimental results and applications: *Jl. Struct. Geology*, **14**, 41-56.

Barton, M. E. Mockett, L. D. and Palmer, S. N. (1993) An engineering geological classification of the soil/ rock borderline materials between sands and sandstones: In Cripps, J. C., *et al*., (eds) The Engng. Geol. of Weak Rock: *The Geol. Soc. Special Publication*, **8**, 125-138.

Bell, F. G. (1978) The physical and mechanical properties of the Fell Sandstones, Northumberland, England: *Engng. Geol*., **12**, 1-29.

Bell, F. G., Culshaw, M. G. (1993) A survey of the geotechnical properties of some relatively weak Triassic sandstones: In Cripps, J. C., *et al*, (eds) The Engng. Geol. of Weak Rock: *The Geol. Soc. Special Publication*, **8**, 139-148.

Bieniawski, Z.T. (1984) Rock Mechanics Design in Mining and Tunneling: *A.A. Balkema*, Rotterdam.

Dick, J. C., Shakoor, A., and Wells, N. A. (1994) A geological approach toward developing a mudrock-durability classification system: *Can. Geotech. J*., **31**, 17-27.

Dobereiner, L. and de Freitas, M. H. (1986) Geotechnical properties of weak sandstones: *Geotech*., **36(1)**, 79-94.

Gamble, J. C. (1971) Durability-plasticity classification of shales and other argillaceous rocks: Ph.D. Thesis, University of Illinois, Urbana.

Geological Society of London (1970) The logging of rock cores for engineering purposes: *Q.Jl. Engng. Geol*., **3(1)**, 1-24.

Gunsallus, K. L., Kullhawy, F. H. (1984) A comparative evaluation of rock strength measures: *Intl. Jl. Rock Mech. Mining Sci. Geomech. Abst*., **21**, 233-248.

Hawkins, A. B., McConnell, B. J. (1992) Sensitivity of sandstone strength and deformability to changes in moisture content: *Q. Jl. Engng. Geol*., **25**, 115-130.

Ho, C. S. (1986) An Introduction to the Geology of Taiwan: explanatory text of the geologic map of Taiwan: *The Ministry of Economic Affairs*, R.O.C., 164p.

Huang, C. S. (1988) No.4 of Taiwan geological map: Central Geological Survey, 46P.

Hugman, R. H. and Freidman, M. (1979) Effects of texture and composition on mechanical behaviour of experimentally deformed carbonated rocks: *AAPG Bull*., **63**, 1478-1489.

International Society of Rock Mechanics (1978) Suggested methods for the quantitative descriptions of discontinuities in rock masses: *Intl. Jl. Rock Mech. Mining Sci*., **15(6)**, 319-368.

International Society of Rock Mechanics (1981) Rock Characterization, Testing, and Monitoring: ISRM suggested methods. Brown, E. T. (ed), *Pergamon*, Qxford, 211p.

Olivera, R. (1993) The Engineering Geology of Weak Rock. In: Cripps, J. C., *et al*., (eds) Weak rock materials: *The Geol. Soc. Special Publication*, **8**, 5-15.

Onodera, T. F, and Asoka, K. H. M. (1980) Relation between texture and mechanical properties of crystalline rocks: *Bull. Intl. Assoc. Engng. Geol*., **22**, 173-177.

Shakoor, A. and Bonelli, R. E. (1991) Relationship between petrographic characteristics, engineering index properties and mechanics properties of selected sandstone: *Bull. Intl. Assoc. Engng. Geol*., **28**, 55-71.

Ulusay, R. Tureli, K., and Ider, M. H. (1994) Prediction of engineering properties of a selected litharenite sandstone from its petrographic characteristics using correlation and multivariate statistical techniques: *Engng. Geol*., **37**, 135-157.

Vutukuri, V. S., Lama, R. D., and Saluja, S. S. (1974) Handbook on Mechanical Properties of Rocks: *Trans. Tech. Publications, Clausthal, Germany*, **1**, 280p.